CHAPTER 3

TRICHLOROACETIC ACID IMPRINTED POLYMER AND INTERDIGITATED CONDUCTOMETRIC TRANSDUCER

3.1. Principle of interdigitated conductometric transducer (Jdanova *et al.*, 1996)

During recent years, biosensors based on microfabricated transducer have been extensively studied. Among them, interdigitated conductometric microdevices offer specific advantages. This transducer consists of a planar glass support with interdigitated gold electrode pairs on one surface in a planar configuration. Conductometric microbiosensors, in comparison with other electrochemical sensors like amperometric enzyme electrodes and EHFETs (enzymatic field effect transistors), do not need of a standard reference electrode which might be troublesome in many practical applications because a reliable reference is a critical issue in miniaturised sensor arrays, and their driving voltage can be sufficiently small to minimize substantially the sensor's power consumption and to reduce safety problems when they are used in vivo. The principle of the detection is based on the changes of the electrical resistance between two parallel electrodes by many biochemical reactions in solution. One major attractive feature of the conductometric detection mode has a advantage that a large number of reactions involve either consumption or production of charged species and therefore, lead to a change in ionic composition of the reacting solution. Therefore, such thin film conductometric electrodes were used to realize sensors sensitive to various target analytes in respect of organic and inorganic substances. From a technological point of view, thin-film metal electrodes are suitable for miniaturization, multisensor network design and production on a large scale using the low cost thin-film technology.

High sensitivity is achieved when interdigitated electrodes are coated with nanostructured thin films ($\sim$ 2 nm thick per deposited layer), which are able to detect very small changes in conductivity and dielectric properties of the materials comprising individual sensing units in contact with a liquid medium.

The ongoing miniaturization of the electrodes led to increasing theoretical and technological attention on the electrode-solution interfacial impedance, whereas less attention was

paid to the resistive part stemming from the electrolyte itself, this being the actual measurand. The cell constant describes the proportionality between the measured resistance and the specific resistance of the electrolyte.

The cell constant K [cm^{-1}] of an electrolyte conductivity sensor is defined as the proportionality factor between the specific resistance ρ [$k\Omega$ cm] of the electrolyte and the measured resistance R_b [$k\Omega$] (Olthuis *et al.*, 1995):

$$R_b = \rho K \tag{3-1}$$

The cell constant is determined by the geometry of the sensor. No description can be found in the literature regarding the resistance R_b, but several papers give a theoretical description of the capacitance between two conductors, even for complex geometries. These theoretical descriptions can readily be used to describe the resistance, because if the capacitance between two conductors is known, the resistance between these conductors is also known under certain conditions, using electromagnetic field theory. For two conductors of arbitrary shape, separated by a dielectric medium with a non-zero conductivity, the following expression can be derived, using Ohm's law and Maxwell's equations, where E denotes the electric field:

$$RC = \frac{\oiint_S \varepsilon_o \varepsilon_r E \cdot dS}{\oiint_S \sigma E \cdot dS} \tag{3-2}$$

where the medium, with conductivity (T [mS cm^{-1}] (= $1/\rho$) and relative dielectric constant ε_r, is isotropic and with R and C the resistance and capacitance between the conductors, respectively. The surface integral is carried out over a surface enclosing one conductor. If in addition the dielectric medium is homogeneous, Equation (2) can be simplified to

$$RC = \varepsilon_o \varepsilon_r / \sigma \tag{3-3}$$

Therefore, if the capacitance between two conductors is known, the resistance can be obtained directly from Equation (3). For two parallel-plate conductors, Equation (3) can be simply checked, because the analytical expressions for R and C of such a configuration are known (ignoring any fringing effects):

$$C = \varepsilon_o \varepsilon_r A/d \quad and \quad R = d/\sigma A (= \rho d/A)$$

thus

$$RC = \varepsilon_o \varepsilon_r / \sigma$$

with d and A the separation and the area of the plates, respectively. By combining Equation (1) and (3) with $R = R_b$, the parameter of interest, the cell constant K, can be expressed in terms of the capacitance:

$$K = R/\rho = R\sigma = \varepsilon_o \varepsilon_r / C \qquad (3\text{-}4)$$

Though they have a lot of essential advantages, interdigitated conductometric biosensors also present some drawbacks. Being based on membrane conductivity changes they cannot work properly in high ionic strength samples. Furthermore, the response of these sensors can be highly dependent on the buffer capacity of the sample. Moreover such biosensors can exhibit narrow dynamic ranges and low sensitivities

3.2. Trichloroacetic Acid Imprinted Poly(Ethyleneglycoldimethacrylate-co-4-vinylpyridine) Modified Interdigitated Conductometric Sensor

3.2.1. Objective

The aim of this chapter was to seek the suitable determination method for haloacetic acids in drinking water by the use of copolymer of ethylene glycol dimethacrylate and 4-vinylpyridine as sensitive material in interdigitated conductometric sensor.

3.2.2. Method

3.2.2.1. Fabrication of the Sensor Device

The sensor devices fabricated in this study were of thick-film type. The gold paste was screen-printed on a pre-cleaned borosilicate glass (1 mm thickness and 15 mm × 20 mm) with a pair of comb-type Au electrodes having interdigitated distances of 0.5 mm and

overall area 11 mm × 8 mm (Fig. 3.1A). This electrode unit was sintered at 550 ^{O}C for 3 h. The thickness after sintering was about 1 μm as measured by an atomic force microscopy (AFM) method. The procedure for immobilization of MIP on electrodes was as follows. TCAA (14 mg, 0.08 mmol) was dissolved in 1 ml acetonitrile. Appropriate amounts of VPD and EDMA were admixed, followed by the addition of AIBN (9 mg, 0.05 mmol). These monomeric mixtures were purged with a stream of nitrogen gas for 1 min, and pre-polymerised at 65 ^{O}C for 1 min in a water bath. The viscous polymer (6 μl) was spread evenly over electrode pattern of the interdigitated conductometric gold electrode placed in a chamber. Subsequently, the chamber was flushed with nitrogen gas for 1 min to remove the radical scavenger oxygen before being closed and oven-heated at 70 ^{O}C for h. After the immobilizing process, the electrode was washed with de-ionized water to remove the template molecules. A non-imprinted polymer (NIP) electrode, which was included as the control, was prepared in the same way as the MIP electrode, but in the absence of the TCAA template.

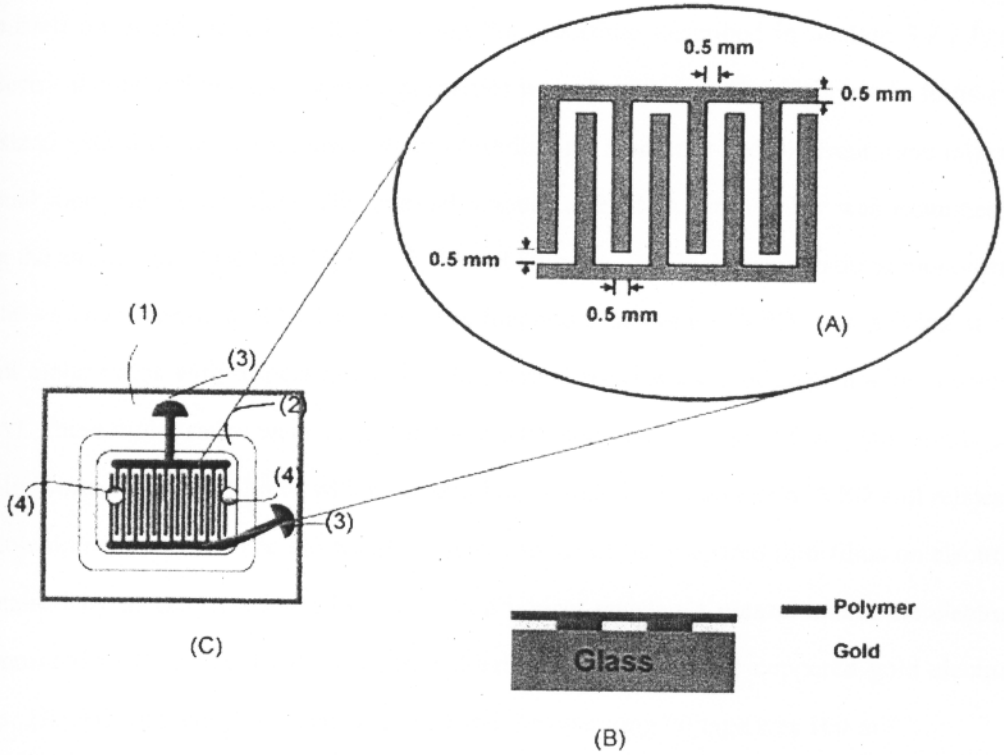

Fig. 3.1. (A) Schematic top view, (B) schematic cross-section of the interdigitated conductometric sensor device, (C) Schematic diagram of the analytical micro-system. (1) Glass support; (2) silicone pad; (3) electrode contact; (4) drilled-through hole.

Elemental analysis the MIP thin-film coated on electrodes was performed on a LV electron microscope equipped with an Oxford Instruments LINK-ISIS 300 X-ray detector and microanalysis system. The morphology of deposited film was inspected by an atomic force microscope (AFM) using a Nanoscope III Scanning tunnel microscope. The thickness of the films (see Fig. 3.1B) was determined by scratching with a needle and measuring depth of the scratches using an AFM with a Nanotec Electrinica WSxM scanning probe microscopy software version 3.0 Beta 8.1.

3.2.2.2. Optimisation of Polymer Composition

The optimal amount of functional monomer and cross-linking monomer required for the manufacture of the MIP film on interdigitated electrode was verified. A set of molecularly imprinted polymer films and the corresponding non-imprinted polymer films were immobilized on interdigitated electrodes using the procedure described in Section 3.2.2.1, and their electrical conductivity and adhesive properties were determined. These polymeric films were synthesized with different initial amounts of cross-linking monomer and different mole ratios of functional monomer to template. The optimal amount of EDMA cross-linker was examined by varying the amount of EDMA as 55, 65, 70, 75 and 80 mol%, while the mole ratio of monomer to template was kept constant at 2:1. Further, the functional monomer (VPD) was applied at five different molar ratios with respect to the template with a fixed amount of cross-linking monomer (EDMA). These molar ratios were 1, 2, 4, 6 and 8 mol monomer to 1 mol of template. In the case of non-imprinted polymer film to which no template is added the amounts of VPD still relates to these stoichiometric ratios. The electrical resistance in air of the prepared thin-films on electrode was obtained by means of a Precision LCR. In a typical resistance measurement, the electrode was connected to Precision LCR meter by soldering copper wires on coppered gold electrode contacts. The AC frequency of 1 kHz was used and the operating voltage was 100 mV.

3.2.2.3. Sensor fabrication

A diagram of the flow-through conductometric sensor system is shown in Fig. 3.1C. The glass plate that constituted the integrated sensor array and wire connections with electrode-contacts, was coupled with a 16 mm × 13 mm, 3 mm thickness home-made silicone pad (obtained from the commercial polydimethylsiloxane and hardener). This silicone pad has a 11 mm × 9 mm × 1 mm depth cavity created by molding. Through holes of 1 mm diameter for sample inlet and outlet were drilled through the cavity. Assembly of the thin-film sensor array with the silicone pad, followed by incorporation into a Perspex housing-box of 4.0 cm × 3.0 cm × 0.4 cm gave the analytical microsystem with a total internal volume of 90 µl. This integrated miniaturised device not only minimised the sample volume, but also considerably reduced the total assay time.

The sampling and conductometric analysis system of the sensor consists of a liquid port for delivery of water sample from a sample-reservoir, a peristaltic pump, a thermo set and the flow-through microcell/integrated MIP sensor incorporated with a conductometric apparatus controlled by a computer program developed in-house. The function of this system was on-line and the minimum sample volume required was 2.5 ml. The stand-alone sensor was operated at a continuous flow rate of 3 ml min^{-1} driven by Ismatec peristaltic pump. The sensor array output signals were monitored using a network analyser, which read the resistance signals from the sensor array with subsequent display on the Laptop screen. The resistance measurement of sensor was performed by applying an alternating potential (100 mV) to the electrodes with a frequency between 100 Hz and 1 MHz. At the initial measurement, the electrical resistance the sensors was measured in de-ionized water as a reference. The measurements were carried out at room temperature ±1 ^{o}C). The signal was allowed to reach a constant value before subsequent addition of the analyte. The sensitivity of the MIP-based sensor was measured as a function of the changes in resistance of the polymer upon exposure to TCAA or other HAA analogs with concentrations from 0.0005 to 500 mg l^{-1}. A control experiment was carried out with the corresponding NIP-based sensor. In addition, technological parameters (operating frequency, temperature and electrolyte) for the sensor were identified with regard to the response to TCAA, using the electrode giving high resistance change with good adhesion of the deposited film as a

model. For the sample measurement using the sensor, the signal response towards the analyte of sensor was reported as R_s, where R_s is the resistance shift response to the addition of known amounts of the analyte of interest. Every experiment was carried out in triplicate on any particular day of experimentation.

3.2.3. Material and equipment

3.2.3.1. Material

Ethylene glycol dimethacrylate (EDMA) and 4-vinylpyridine (VPD) (Fig. 3.2) were purchased from Aldrich Chemical Company (Mil-waukee, WI, USA). These chemicals were purified by distillation under reduced pressure before use.

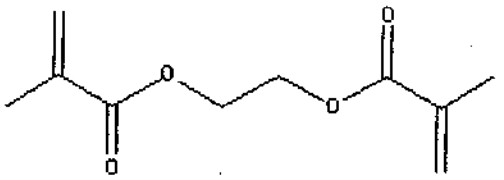

Ethylene glycol dimethacrylate (EDMA) cross-linker

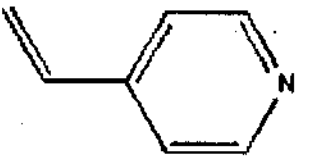

4-Vinylpyridine (VPD) functional monomer

Fig. 3.2. The cross-linker and functional monomer used to prepare acrylate type polymer

2,2-Azobis-(isobutyronitrile) (AIBN) was obtained from Janssen Chimica (Geel, Belgium) and its molecular structure is shown below (Fig. 3.3)

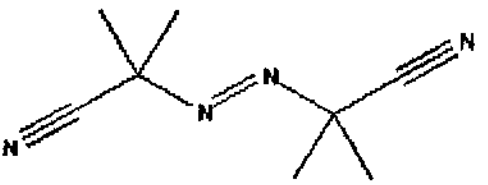

Fig. 3.3. 2,2-Azobis-(isobutyronitrile) initiator

Polydimethyl-siloxane and hardener (Sylgard 184) were obtained from Dow Corning Corporation (MI, USA).

Trichloroacetic acid (TCAA) was purchased from Merck K.G. (Darmstadt, Ger-many). Dichloroacetic acid (DCAA), monochloroacetic acid (MCAA), dibromoacetic acid (DBAA), monobromoacetic acid (MBAA), tribromoacetic acid (TBAA) and malonic acid were obtained from Fluka Chemie AG(Buchs, Switzerland).

All chemicals for preparing buffer solution (K_2HPO_4, NaH_2PO_4, NaCl, HCl and KCl) were analytical grade and were obtained from Merck (Darmstadt, Germany).

All solvents used in this work were analytical grade and were dried with 4 A pore sized molecular sieve before use. Working standard solutions were prepared daily.

3.2.3.2. Equipment

Atomic force microscope (AFM) (Digital Instru-ments Inc., Santa Barbara, CA) (Fig. 3.4) using a Nanoscope III Scanning tunnel microscope was used to inspect the morphology of deposited film. AFM (Digital Instruments, CA, USA) with a Nanotec Electrinica WSxM scanning probe microscopy software version 3.0 Beta 8.1 (Digital Instruments, CA, USA) was utilized to determine the thickness of the films scratching with a needle and measuring depth of the scratches.

HP 4254A Precision LCR meter (Hewlett Packard, Germany) (Fig. 3.5) was employed to measure the electrical resistance of the thin-films polymer coated electrode.

Ismatec peristaltic pump (MCP-Process Series, Ismatec SA, Wertheim-Mondfeld, Germany) was used to drive the sample solution into the flow cell (Fig. 3.6).

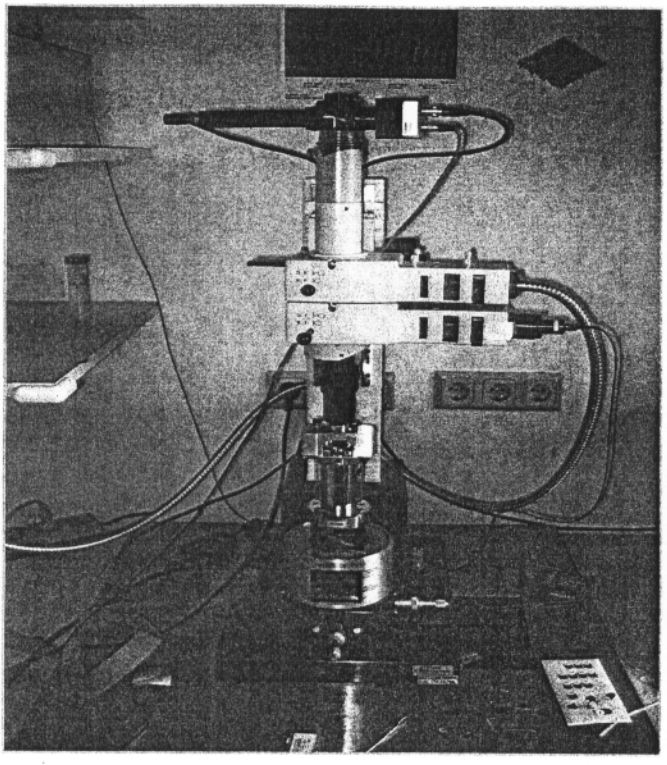

Fig. 3.4. Atomic force microscope (AFM)

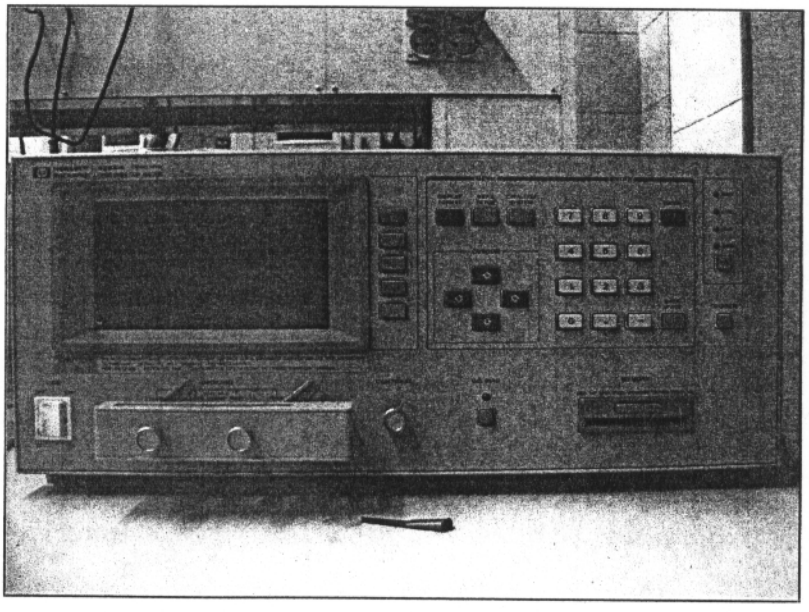

Fig. 3.5. A HP 4254A Precision LCR meter

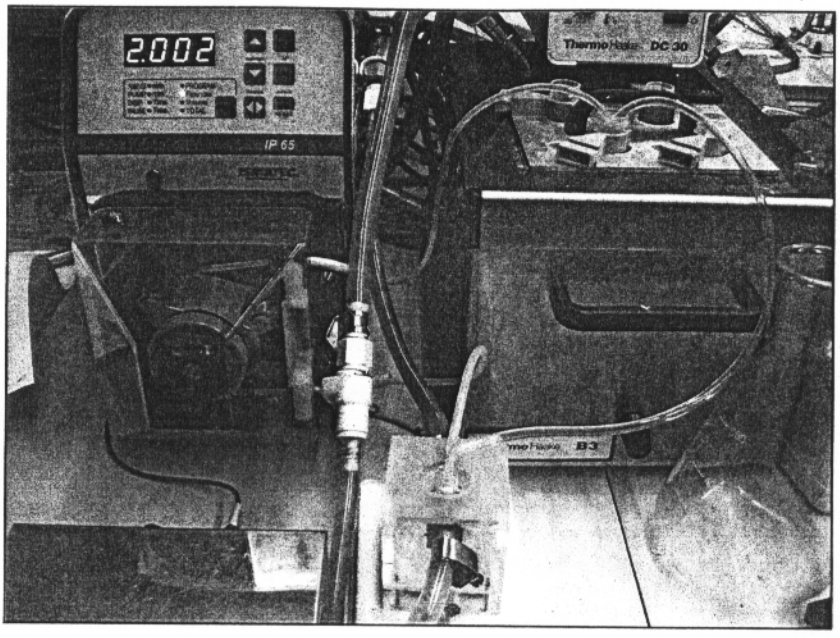

Fig. 3.6. A MCP-Process Series Ismatec peristaltic pump

3.2.4. Results and discussion

3.2.4.1. The MIP-based electrode-fabrication of the sensor device

The polymerization initiator of this study was AIBN, which this compound is suitable for preparation of polymer film on the electrode surface by thermal polymerization. Since this organic initiator can break down as active radical readily at high temperature environment to commence the reaction. The thin-film of polymer generated on the gold electrode surface was the hydrophobic semi-electrically conducting of poly(EDMA-*co*-VPD) and can be tailor-made selective for haloacetic acids by using TCAA as the imprint molecule during polymerization. Ethylene glycol dimethacrylate (EDMA) was chosen as the cross-linking monomer because this cross-linker can form dense rigid network structure and contribute the strength to generated polymer. Subsequently, the produced imprinted hole which was a part of polymer structure correspondingly gained the stable and rigid characteristics. 4-Vinylpyridine (VPD) was utilized as functional monomer for creating imprinted cavity selective to TCAA, since its functional group (amine moieties) was able to form a strong interacted complex with the carboxylic group of TCAA which so called charge-transfer complex. In addition, the insulating

layer of poly(EDMA-*co*-VPD) can be usefully become the continuous conducting phase from this complex. The detection of signal transport from the polymer bulk through the electrode surface with this conducting phase was possible.

To study the immobilization strength of both MIPs and NIPs layer on the surface of interdigitated gold electrodes, the resistance changes before and after complete saturation of polymer layer immersed in the water were comparatively monitored. At dry state, both MIP and NIP layer can provide detectable signal upon measuring with the prepared conductometer. The effect of cleaning process of both MIP and NIP with deionized water on resistance change of coated electrode was studied. Initially, a monomer:template mole ratio of 2:1 and 65 mol% EDMA was chosen to prepare a thin-film of both MIP and NIP coating on electrode surface. After finishing polymerization, the coated electrodes were left cool down to room temperature before being immersed in 100 ml water. At every hour of electrode soaking in water at ambient temperature, resistance measurements of electrodes were carried out in open air. The washing process of polymer coated electrodes was kept constantly until their stable resistance signal can be obtained, which observed after nearly 4 h of washing. The overall resistance changes of both MIP and NIP in air (ΔR_a) were elucidated with making calculation from the resistance value received at the initial and at the end of washing process. A net increase in electrical resistances of the MIP and NIP films coated on electrode surface were observed after 4 h immersion in water to complete saturation of the detected signal. An increase from 2.7×10^8 to 7.6×10^8 Ω represented for the MIP film and the electrical resistance of NIP layer increased from 6.9×10^8 to 8.5×10^8 Ω. Based on the changed electrical resistance value obtained, the ΔR_a of MIP (4.9×10^8 Ω) was almost three times higher than that of the NIP (1.6×10^8 Ω). The alteration in resistance of MIP may be mostly attributed from the removal of template along with the washing water. And the getting rid of some parts of non-polymerized monomers and unconnected polymer from the electrode surface may be the other factor additional responsible on changed resistance. After washing with water the MIP film expressed the higher electrical resistance (lower conductivity) than un-treated layer. This can be evidently described as follows, as the template was continuously removed by the water the conductivity signal of MIP film was gradually declined. This implied that the interaction of template in imprint site was responsible for initial electrical conductivity of MIP layer before template extraction. The change in charge

transfer interactions of TCAA and polymer proportionally determined the change in conductivity of MIP films. Occurrence of charge transfer complexes between the MIP and TCAA at imprint site was evidently confirmed by an emerald-green coloring of polymer film which only generated in case of the MIP after polymerization and these interactions was able to be eliminated by washing with water. These colored complexes were presumably believed arising from the increased conjugated double bond inside polymer structure at imprint site, due to induced alteration of polymer structure suitable to bind with template. This revealed that after polymerization and in the dry state, poly(EDMA-*co*-vinylpyridinium) existed in the form of acid–base complexes of TCAA and VPD monomer. After washing, the impairment of charge transfer complexes at imprint site caused the resistance signal of MIP increased. The signal changes in case of NIP were probably arisen owing to only the removal event of un-reacted monomers and some parts of the non-adhered polymer. The template molecules were omitted in case of NIP during polymerization process. The function group of base polymer, vinylpyridine moieties, was therefore not induced as in quaternized form with carboxylic group of template to create the imprint site in the polymer network. The changed color of polymer film attributing to charge transfer complexes formation was not observed. The difference in electrical resistance changed deriving from both MIP and NIP after washing process revealed the signal change from template removal from the imprint and hence, the possible expected recognition process subsequently manifested. The electrodes fabricated with either MIP or NIP film, either before or after washing in water, gave a resistance signal higher than the bare electrode ($R_a = 7.5 \times 10^3\ \Omega$). This suggested the improved conductivity of the coated electrode after covering the surface with polymer layer having higher electrical conductivity comparing with bare electrode.

The polymer morphology after washing with water was performed using AFM as can be seen in Fig. 3.7a and b. The AFM topology of both MIP and NIP was obviously shown by using contact mode. AFM topographies of the MIP-film surface exhibited more ridges and roughness, while smoother and more uniform coating was represented for the NIP film. These characteristics suggested the influence of template on the different morphology of MIP comparing with NIP film which was prepared in an absence of template molecule.

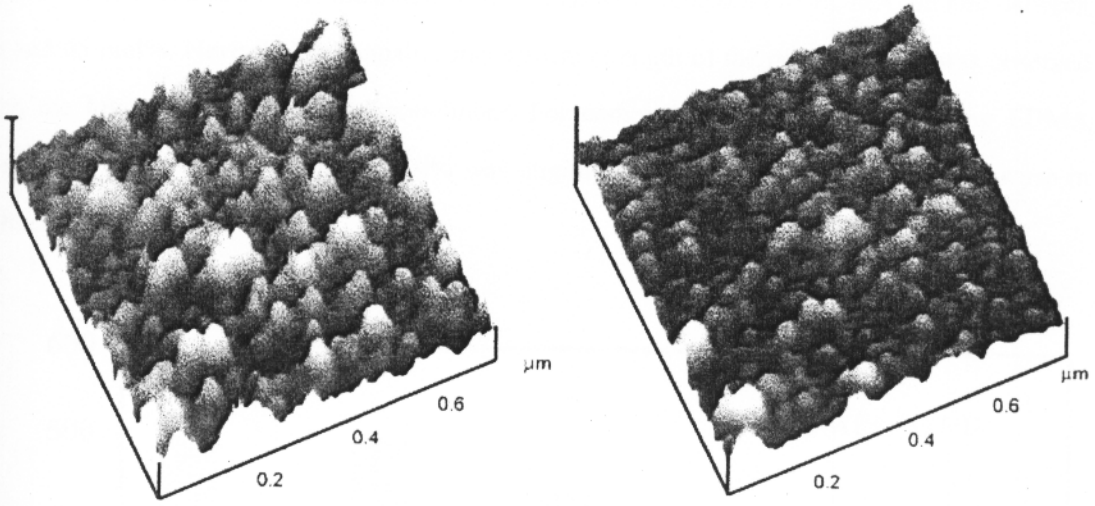

(a) (b)

Fig. 3.7. Three-dimensional AFM images of: (a) MIP and (b) NIP thin-film prepared with 2:1 monomer:template ratio and 65 mol% EDMA (after washing with water for 4 h).

3.4.4.2. The MIP-based electrode-optimisation of polymer composition

The stoichiometric ratio of each monomer in polymer layer may possibly determine the various properties of imprinted polymer including the recognition ability. In order to gain the MIP having optimum properties, the composition of MIP film was therefore explored by focusing towards the basis of resistance change. The change in resistance signal of the MIP was performed concurrently with corresponding NIP to compensate the obtained resistance signal from environmental interfere. By this the resistance change of MIP due to the template removal process was separately elucidated. Besides, the recognition efficiency of MIPs implying from imprint ability was revealed by comparing the change in resistance between MIP and NIP. Fig. 3.8 expressed a dependency of cross-linker amount on the degree of the measured ΔR_a for MIP, while there was no the similar evidence for NIP. MIP producing with lower concentrations range of EDMA (55, 65 and 70) manifested a higher resistance change than those of MIP using higher concentrations of EDMA (75 and 80). The imprinting factor was calculated from the ratio of R_a of MIP-based electrode to R_a of NIP-based electrode after washing in water for 4 h. This content measured the imprinting specificity of MIP comparing with corresponding NIP towards the

template and it attained to the maximum value when MIP composed of EDMA amount between 55 and 65 mol%. Nevertheless, impairer mechanical strength of the polymer layer was observed with the low content of EDMA cross-linker. For compromising reason, a promising EDMA content of choice regarding on 65 mol% was eligibly represented to create the MIP for use in further investigations.

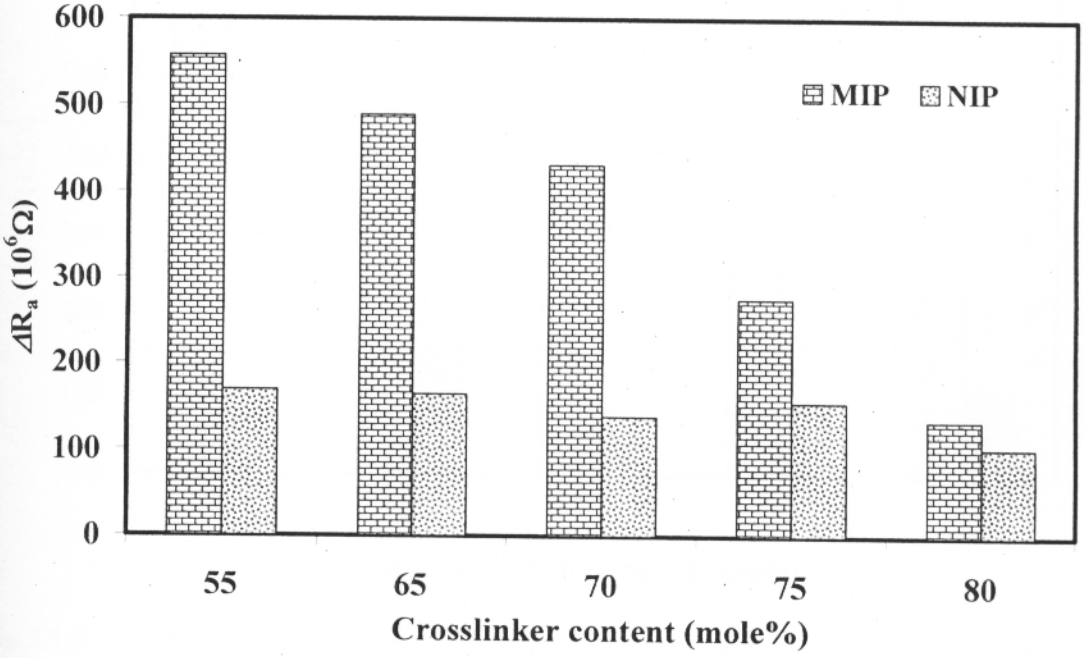

Fig. 3.8. Effect of the amount of cross-linking monomer (EDMA) on the resistance responses of the MIP and NIP thin-film after 4 h exposure in water. Measurements were carried out at 1 kHz and at room temperature. The functional monomer to template ratio of 2:1 was used.

The influence of mole ratio of monomer and template on resistance change of MIP comparing parallely with NIP was investigated by varying the mole amount of monomer on the fixed mole amount of template as shown in Fig. 3.9. The results revealed that the electrical resistance of MIP decreased with an increase in the molar ratio of VPD to template. In contrast, the resistance of NIP was absolutely independent from the varied monomer:template mole ratio. Imprinting factor reflecting the recognition efficiency by MIP was attained to optimal degree of 5.8 at a mole ratio of VPD : template of 1:1. This implied that the VPD moiety at binding site of

MIP preferred to form complexes through 1:1 mole with the TCAA molecules. Although a 1:1 monomer:template ratio showed a favored imprinting factor, but the higher durability and stability of polymer film was achieved by composing with 2:1 monomer:template ratio.

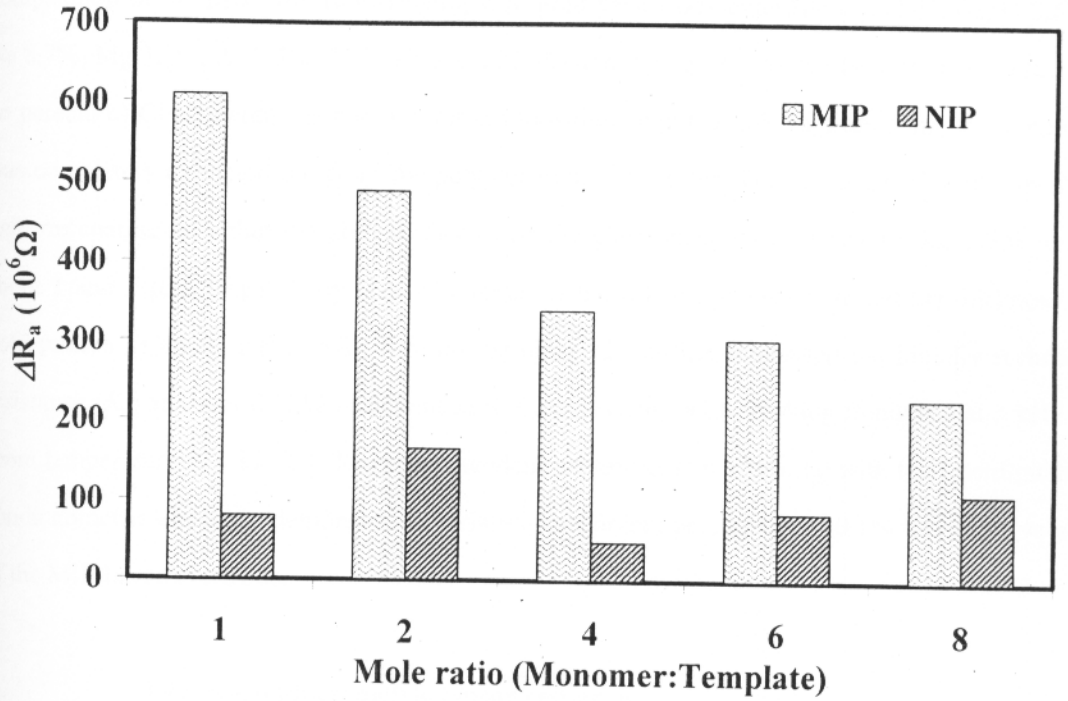

Fig. 3.9. Effect of the amount of functional monomer (VPD) on the resistance responses of the MIP and NIP thin-film after 4 h exposure in water. Measurements were carried out at 1 kHz and at room temperature. The cross-linker content of 65 mol% was used.

From this investigation, the interpreted data indicated that the mole ratio of functional monomer:cross-linker determined the physical property of the film, and a MIP film with a good physical properties can be obtained by composing with 2:1 monomer:template mole ratio, which was found as most promising ratio, and 65 mol% content of EDMA. Advantageously, a relatively higher value of imprinting factor of 4.4 was affordable at the 2:1 monomer:template mole ratio. A good and reproducible of polymer coating was evident from the low relative standard deviation (2.6%, n = 3) obtained. For the technological aspect, the film coating having a compromisingly optimum properties in terms of good stability and high recognition ability to the template achieved from employing 2:1 monomer:template ratio and 65

mol% EDMA was suitably chosen to construct as the recognition layer for the development of conductometric sensor sensitive to HAA for the on-line fashion of HAA analysis.

The completion of template removal process was subsequently confirmed with elemental analyses of MIP thin-film laying on gold electrode by using SEM. An elemental composition of the MIP film (underlaying with gold paste) was elucidated as C 45.9%, O 3.6%, Na 8.7%, Mg 3.0%, Al 1.3%, Au 0.10%, Ca 22.3% and Ag 15.1%. As can be seen that, there was no percent of Cl elemental appeared in the composition acquired, this suggested that the template was completely extracted out from the polymer bulk with water. The thickness of MIP thin-film uniform coating on either the gold surface or on the glass surface was derived using AFM to be about 1 and 2 μm, respectively. The difference of these two numbers revealed the thickness of gold pattern as about 1 μm. MIP film on the electrode surface expressed the initially recorded resistance (R_0) at about 80 kΩ in deionised water measuring with working frequency at 3 kHz at room temperature (24 ±1 ^{O}C). Three independent experiments performing with the interdigitated conductometric electrode demonstrated variation coefficient percentage of 0.1% for the R_0 values of the MIP-based electrode.

3.4.4.3. Conductometric sensor response

Ordinarily, the connection of polymeric film and solution relies on like dissolves like rule. The hydrophobic polymeric film is difficult to get wet and penetrate with a high polar solution. It may be finally de-attached from the surface where the film is coated. MIP films constituted from hydrophobic cross-linker (EDMA) perfectly obeyed this rule when come to contact with high polar water (comparing with the other organic solvents). Advantageously, MIP films prepared with poly(EDMA-*co*-4-VPD) as polymer material and TCAA as template afforded a good properties in terms of adhesion and strength in aqueous medium. The sensitivity of the sensor, integrating with this MIP, to the analyte in aqueous medium was expressed in a few ten seconds range (30 s) and the sensor consumed the time to get constant response not longer than 2 min. The proposed MIP conductometric sensor demonstrated the somewhat fast response time comparing with the published composite MIP conductometric sensor which constructed with membrane electrode. The latter gained the longer response time in the order of 30 min. The

transducer part and the sensing layer of the sensor may be the key factors taking responsibility for this rapid response of this MIP conductometric sensor. Consequently, the sensing layer behaving as chemical receptor was very closely located on the surface of transducer part composing from interdigitated array electrode. This characteristic caused the rapid diffusion of analyte or transduction of signal to the transducer system and hence, the measurement can be quickly accomplished (Tomcik *et al.*, 2006). TCAA template was easily penetrated into the MIP layer due to induced higher polarity of poly(EDMA-*co*-VPD) network when closely encounter to the template. And the intrusion of aqueous medium may also be promoted with this changed characteristic of poly(EDMA-*co*-VPD) leading to an more easily penetration of TCAA into polymer matrix. The MIP sensor responded with template more rapidly than that of NIP sensor, this was because the water can penetration into the MIP matrix more easily than the NIP film.

The influence of continuously added TCAA solution at various concentrations into MIP sensor on the resistance response of the sensor was investigated and shown in Fig. 3.10. The results showed that the resistance of MIP sensor rapidly decreased with each drop of TCAA solution and also, the proportional relationship of resistance response of the sensor and TCAA concentration was observed. While the resistance changes of NIP sensor were negligibly affected with increased concentrations of TCAA. The different signal response of MIP and NIP-based sensor in aqueous medium was revealed, this suggested the measurement of sensor response could be performed in this medium due to interaction between MIP and TCAA was not disturbed. In addition, resistance of prepared sensor did not appear to be influenced considerably with non-specific binding. In order to gain insight binding mechanism of TCAA to the imprinted site, it was worth to explain the increase in conductivity of sensor upon inclusion of TCAA into created cavity in terms of concerned phenomena as followed. In an aqueous solution, MIP was reasonably prohibited to form hydrogen bonding with TCAA functional group. For this the interfering of water molecule may be a reason. Ionic interaction between the carboxylate ion of TCAA and ionized form of functional monomer was without any doubt responsible to be main source of binding force between MIP and TCAA in aqueous solution. The already mentioned charge transfer complexes inside MIP may be generated from the ion-pairs between TCAA ions and the vinylpyridinium ions of the imprinted cavity. Consequently, the overlap of electron π-orbitals between host (MIP) and guest molecule (TCAA) in charge transfer complexes led to

extended conduction and valence bands of complexes when compared with the each original molecule, causing the conductivity of the MIP film changed (Oison *et al.*, 2004).

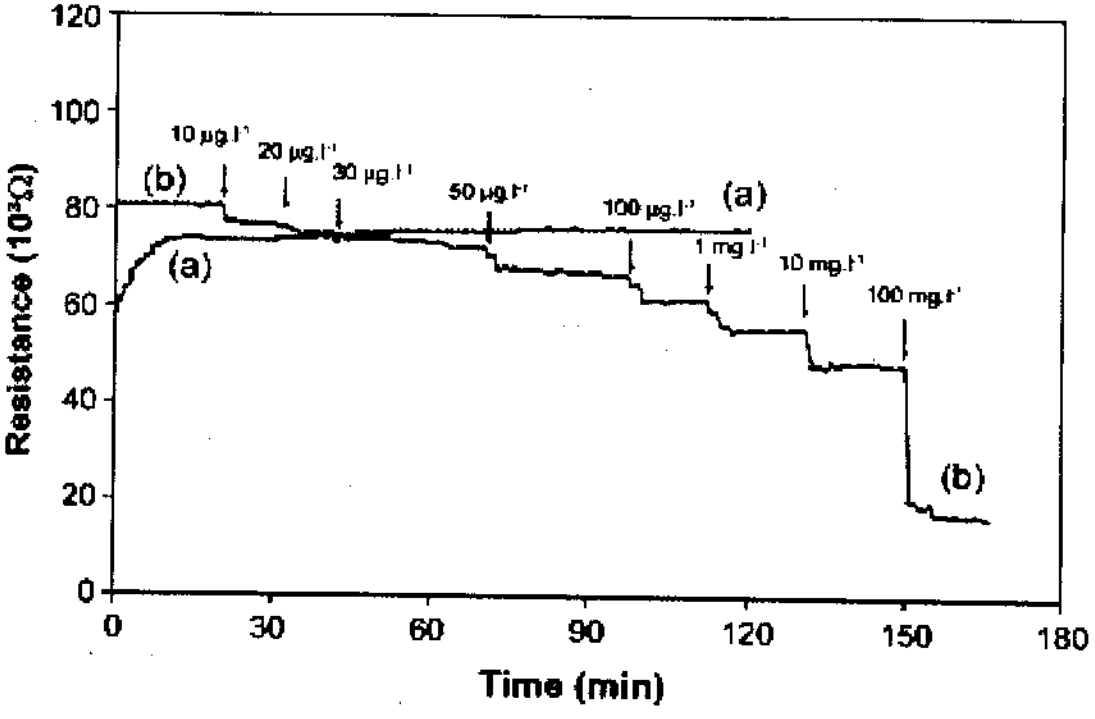

Fig. 3.10. Signal response of: (a) reference sensor and (b) MIP sensor to subsequent additions of TCAA at 1 kHz.

3.4.4.4. Effect of experimental parameters on the sensor signal

Many experimental factors i.e. applied frequency, temperature and electrolyte substances were presumably believed to affect the conductivity response of MIP-based sensor which composed of semi-conducing polymeric film as sensing material. Therefore the effect in variation of these factors on signal response of sensor should not be omitted to be explored.

A. Effect of applied frequency

An ac frequency value between 0.1 and 1000 kHz was chosen as applied frequency range to study its effect on the resistance changes of MIP-based sensors responded to TCAA concentrations in the range of 0 to 70 μg l^{-1} in aqueous solution. As can be seen in Fig. 3.11, the electrical resistance of the sensor consequently decreased with increasing in the applied frequency at all concentrations of TCAA studied (0-70 μg l^{-1}). The process of electron percolation in the cross-linked poly(VPD-*co*-EDMA) may be manifested by measured resistance response of sensor at lower frequencies as can be seen in Fig. 3.11. The resistance of the sensor obtained was susceptible on the applied frequency variation and also, the presence of TCAA molecules contained in the solution.

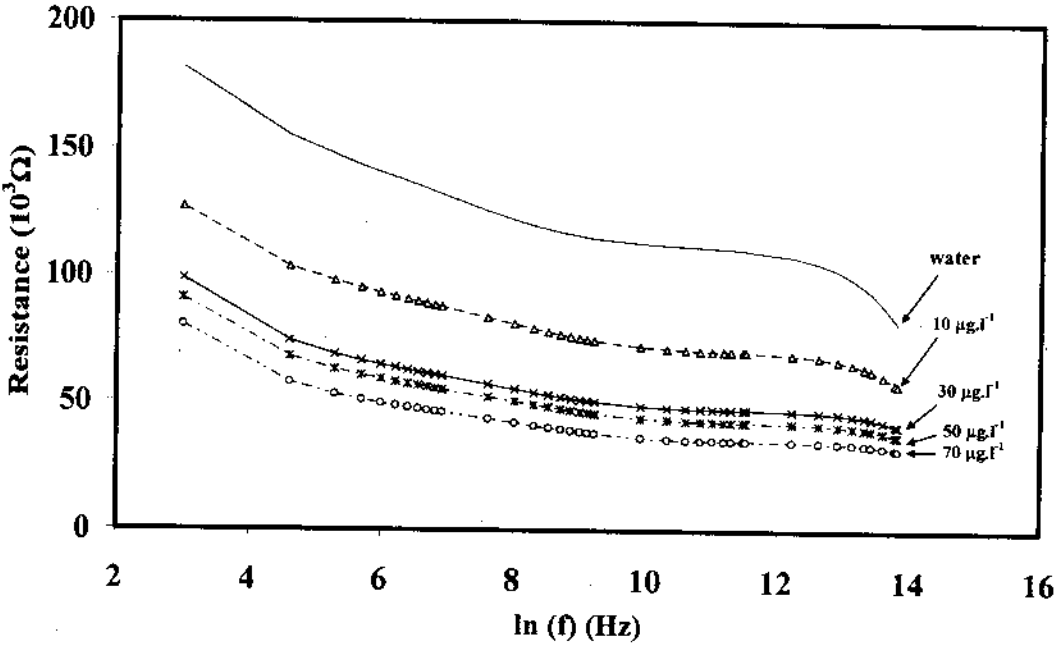

Fig. 3.11. Effect of the ac frequency on the resistance responses of the MIP sensor at various concentrations of TCAA. Measurements were carried out at room temperature.

The incremental addition of TCAA solution caused the alteration of resistance of MIP IDC sensor narrower at high frequency region when compared at low frequency range. The sensor measured in the ac frequency range of 1-10 kHz expressing a reasonable

resistance response to TCAA solution. Thus, the frequency of 3 KHz was selected as operating frequency for performing the all further experiments of prepared sensor.

B. Effect of experimental temperature

The temperature fluctuation of sensor system may affect the way of IDC sensor responded to TCAA solution. Therefore, the changes in experimental temperature on the resistance response of the sensor were investigated over the temperature range of 299–333 K in expected binding saturation of the imprinted cavity with excess amount of TCAA (200 $\mu g\ l^{-1}$) as demonstrated in Fig. 3.12.

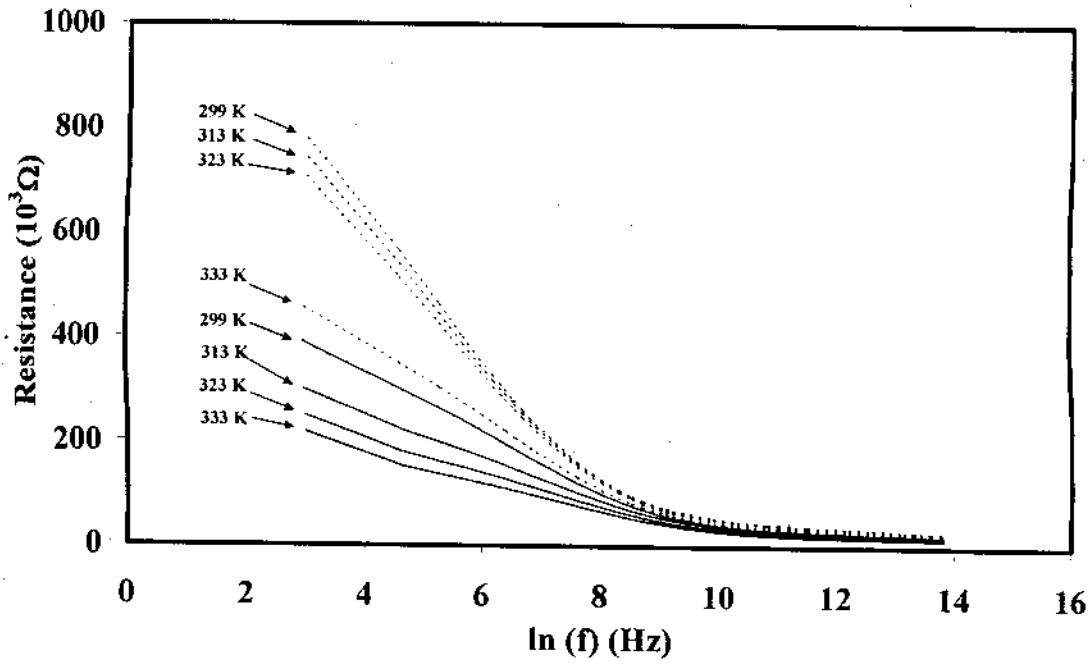

Fig. 3.12. Effect of temperature on the resistance response upon 200 $\mu g\ l^{-1}$ of TCAA for: reference sensor (dashed lines) and MIP sensor (thick lines), at various frequencies.

It was found that the resistance response of MIP IDC sensor gradually declined when temperatures increased in the range of 299 to 333 K. On the other hand, the resistance response of NIP IDC sensor was negligibly affected from the increased temperature from 299 and 323 K. At the elevated temperature 333 K caused the resistance of the both MIP

and NIP sensor attaining the comparable level and a very slight resistance difference of both sensors was obtained due to the polymer volume was obviously expanded allowing the penetration of water through polymer films occurred completely. Owing to MIP and NIP films were composed of the same polymer structure, poly(EDMA-co-VPD), and as the template omitted in the NIP composition, the distinction of resistance response between these two sensors was certainly due to the imprinting effect of the binding site and TCAA template.

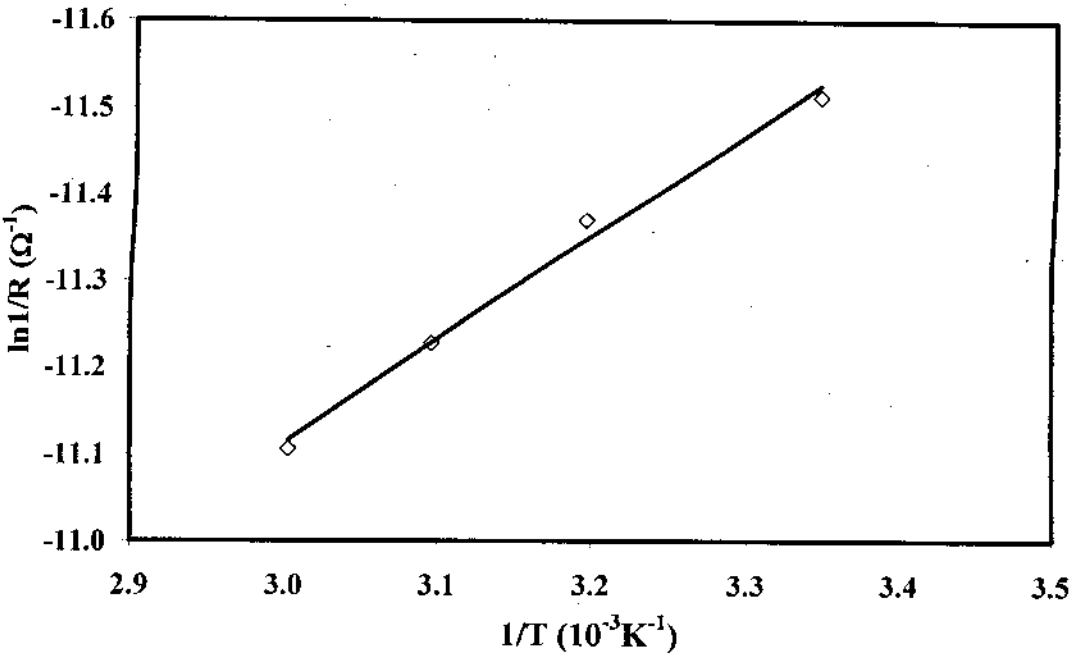

Fig. 3.13. Arrhenius plot for the electrical conductivity of MIP electrode.

The electrical resistance of MIP IDC sensor follows the Arrhenius equation illustrated below.

$$\frac{1}{\Omega} = A\exp\left(\frac{-E_a}{RT}\right)$$

where A is the pre-exponential factor, E_a represents the activation energy, R the gas constant and T is the temperature. As can be seen in Fig. 3.13, at 35 K higher than the ambient temperature, the lower resistance from 10^5 to 10^4 Ω of the MIP-based sensor was observed. This suggested that the synthesized MIP showed semi-conductive property due to the π-type conjugative moieties within polymer matrix. An alteration of charge-transfer interaction as temperature varies may be

the key factor responsible for changed resistance of the MIP sensor upon the changed temperature. The calculated activation energy, 10.2 kcal mol^{-1}, of resistance of MIP sensor depending on altered temperature was obtained from the Arrhenius equation, may be possibly related with the excitation energy of thermal generation concerning with charge-transfer interaction of binding site in the polymer. The overall results suggested that the sensitivity of the sensor was strongly governed with the temperature deviation. For this reason, the measurement of this prepared sensor should be taken place under good controlled constant temperature.

C. Effect of electrolytes

The TCAA normally exited together with several electrolytes in water resources and these ionic substances may subsequently be still contained in the drinking water even though upon passing home water treatment system. Therefore, the influence of the electrolyte on the resistance shift response of the prepared sensors should be explored. The results revealed that the order of the resistance shift response of both MIP and NIP IDC sensor to sample solution containing TCAA of 200 $\mu g\ l^{-1}$ increased with an increase in NaCl concentration. As can be seen in Fig. 3.14, the resistance of both MIP and NIP IDC sensor concurrently decreased when disclosed to the analyte (TCAA) and electrolytes (NaCl) can be described according to the abundant of analyte and counter ions-behaved ionic substances in the polymer layer. This caused the gold electrode surface in the sensing device was covered with a high concentration of charged species. It was found that MIP sensor was seemed to persistently express the higher resistance changes than that of NIP sensor when exposed to the sample solution initial containing 200 $\mu g\ l^{-1}$ TCAA at every electrolyte concentration studied. Further addition of the electrolyte did not appear to have effect with this constant response gap. This constant resistance response difference of MIP and NIP sensor in the NaCl concentration range between 0.2 and 3.4 mg l^{-1} (0.01–200 mM) suggested that the affinity of the MIP IDC sensor with the TCAA was not obviously influenced with the incremental concentration of NaCl.

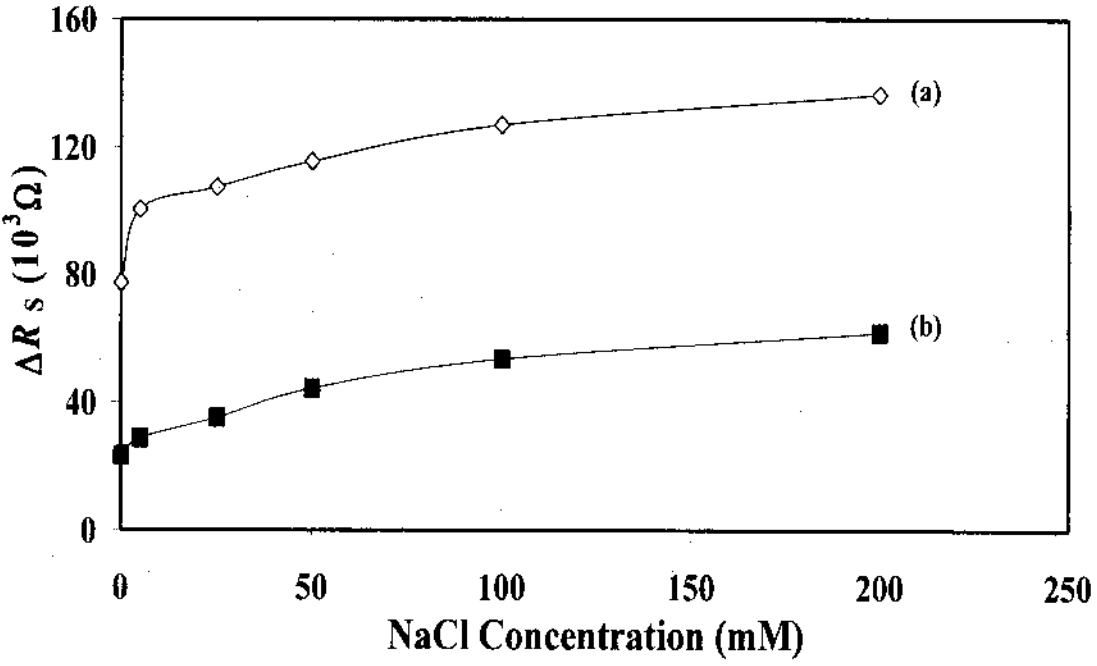

Fig. 3.14. Effect of NaCl on the resistance shift response of (a) MIP sensor and (b) reference sensor at 3 kHz and at room temperature. Responses were initiated by the addition of 200 μg l^{-1} TCAA.

3.4.4.5. Concentration dependence on signal response of sensor

The signal response characteristic of the prepared sensor as the magnitude of analyte concentration increased was examined using TCAA concentrations in the range of 0-500 μg l^{-1} as can be seen in Fig. 3.15. At concentrations of TCAA below 100 μg l^{-1}, the increased concentration of TCAA gave the higher signal response of MIP sensor, while NIP sensor revealed slightly changes of signal response when exposed to the same range of TCAA concentrations studied. The response of MIP sensor appeared to still be constant using concentrations of TCAA higher than 100 μg l^{-1}, while the signal response of NIP sensor was continuously kept consistency. The saturation of the recognition cavities by imprint molecule was probably responsible for this result. This was evident, in case of MIP, the target analyte was definitely included to the recognition sites in the MIP film. The absorption behaviour to analyte of the MIP film incorporated in sensor can be relied to the Langmuir isotherm expressed as

$$\Omega = \frac{\Omega_{max} Kc}{1 + Kc}$$

where Ω_{max} is the maximum value of the resistance response (Ω), K represents the modified adsorption equilibrium constant and c is the concentration of the analyte. A straight line with a single apparent binding constant of 9.3 μM^{-1} can be achieved by plotting of $1/c$ versus $1/\Delta R_s$. The cross-linked polymer templating with TCAA showed the affinity for its initially added template molecule during polymerization was comparable to those of the other MIPs published in literatures (Sergeyeva *et al.*, 1999; Liao *et al.*, 2004).

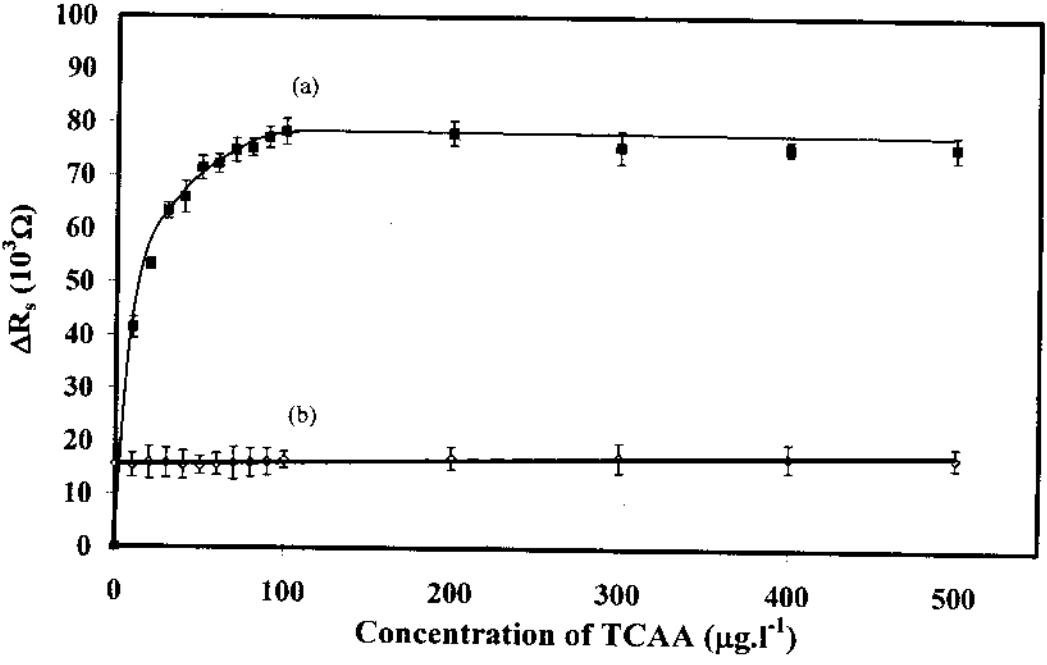

Fig. 3.15. Concentration dependence of the sensor response to TCAA for: (a) MIP sensor and (b) reference sensor. Each point represents the average of three independent measurements. Measurements were carried out in distilled water at 3 kHz and at room temperature.

3.4.4.6. Analytical characteristics

The proper results in case of analytical characteristics of prepared MIP IDC sensor to TCAA and various TCAA analogs can be obtained from calibration curves deriving from the resistance shift parameter dependency. The shift resistance of the MIP sensor

was proportionally related with the logarithm of the concentrations (log c) with a good correlation coefficient ($R^2 > 0.97$) of TCAA in the range of 0-100 μg l^{-1}, and the other five HAAs (DCAA, MCAA, TBAA, DBAA and MBAA) in the range of 1-500 μg l^{-1}, depending on the compound, and the mixture of total six HAAs in the range of 10-400 μg l^{-1}. The calibration data are tabulated in Table 3.1. The obtained limits of detection was calculated according to $3S_b/m$ basis, S_b were approximated as the average standard deviation (n=3) of the signal response for HAAs, where m is the linear calibration of a straight line, were in the range of 0.5-5 μg l^{-1} for the various HAAs. A maximum permissible contamination level of 60 μg l^{-1} has been issued by the US Environmental Protection Agency (USEPA) for the five normally occurring haloacetic acids including TCAA, DCAA, MCAA, DBAA and MBAA of the regulation for disinfection by-product. This contamination level has been adjusted to the lower value in the next coming years to be 30 μg l^{-1}. The requirement of regulation comprised of DCAA should never be existed, and 30 μg l^{-1} TCAA was the highest concentration containing in the sample. Thus, the concentrations well below the maximum permitted concentrations of HAAs can be detected with the MIP.

Table 3.1

Calibration data obtained for the analysis of TCAA and five other HAAs by the MIP sensor

Compound	Slope	R^2	Working range (μg l^{-1})	LOD (μg l^{-1})
TCAA	38.89	0.992	0-100	0.5
DCAA	27.17	0.993	1-500	1.2
MCAA	24.17	0.986	5-500	5.0
TBAA	5.81	0.972	10-500	5.3
DBAA	5.63	0.985	40-400	1.7
MBAA	11.2	0.987	30-400	1.2
Six HAAs[a]	117.23	0.980	10-400	5.0

[a] Refers to TCAA, DCAA, MCAA, TBAA, DBAA and MBAA altogether.

Stability of the developed sensor was a factor showing whether the sensor had high economic impacts. For this repeated measurements of the MIP IDC sensor signal

response towards HAAs were carried out in order to examine the persistency of the prepared MIP electrode. It was found that more than 50 times of repeated analyte determination with reliably reproducible detection signals can be accomplished by using single MIP electrode and the electrode could be advantageously kept at room temperature more than 3 months without observing any impairment of sensor sensitivity.

3.4.4.7. Selectivity of the sensor

To evaluate the whole selectivity of the MIP electrode, the effects of structurally related haloacetic acid compounds such as DCAA, MCAA, TBAA, DBAA, MBAA and non-haloacetic acid compounds such as malonic acid and acetic acid, on sensor conductivity were examined. As can be seen in the Fig. 3.16, electrical resistance signal of MIP sensor responded in very slight content upon exposure to non-haloacetic acid compounds, either acetic acid or malonic acid, in the concentration range of 10-500 $\mu g\ l^{-1}$ (see Fig. 3.16). In contrast, shift of the resistance signal of the MIP sensor was significantly affected with an increasing in concentrations of structurally related haloacetic acid compounds. This suggested that the imprint cavities were produced exactly complementary with target TCAA template within MIP coating on the electrode surface. Consequently, the affinity of prepared polymer was highest for TCAA. The other HAA analogues, having some part of structure similar to TCAA, were able to fit into recognition site in different degrees. Therefore, the difference of induced resistance changes of MIP was expectedly obtained. The results additionally revealed that both structurally related haloacetic acid and non-haloacetic acid compounds caused the resistance response of NIP sensor negligibly changed (data not shown). By plotting the various concentrations of analogs versus signal response of the sensor, calibration curves of all analogs were constructed as shown in Fig. 3.16. The results demonstrated that the MIP sensor responded to all chloro-substituted HAAs at reasonable sensitivity (incline of calibration curve slope), but the responses of MIP sensor to the bromo-substituted HAAs were obviously lower. The considerable bigger atomic size of bromide comparing with chloride atom was presumably responsible for harder inclusion into binding site in case of former analogs. By making comparison between the value of maximum resistance response of MIP sensor obtained for all analogs relatively to that for TCAA, the selectivity figure

of the sensor to all analogs was exposed. The results indicated that the selectivity of sensor for HAA was correspondingly related with either electronegativity or size of analogs, the weaker electronegativity or larger molecule of HAA existed the decrease in sensor selectivity was received. The combination of size and shape of halogen atom located in all analogs relatively compared with template imprinted cavity which based on ion-ion interaction may be the dominant factor governed the specificity of MIP sensor in respect to all analogs. The DCAA showed the highest selectivity value with the MIP sensor (94%), but the MIP sensor also significantly responded for MCAA (93%), MBAA (84%), TBAA (78%) and DBAA (66%). This implied that the assay with developed sensor showed the group specificity rather than analyte specificity and this determination method was therefore advantageously used to detect this group of HAAs.

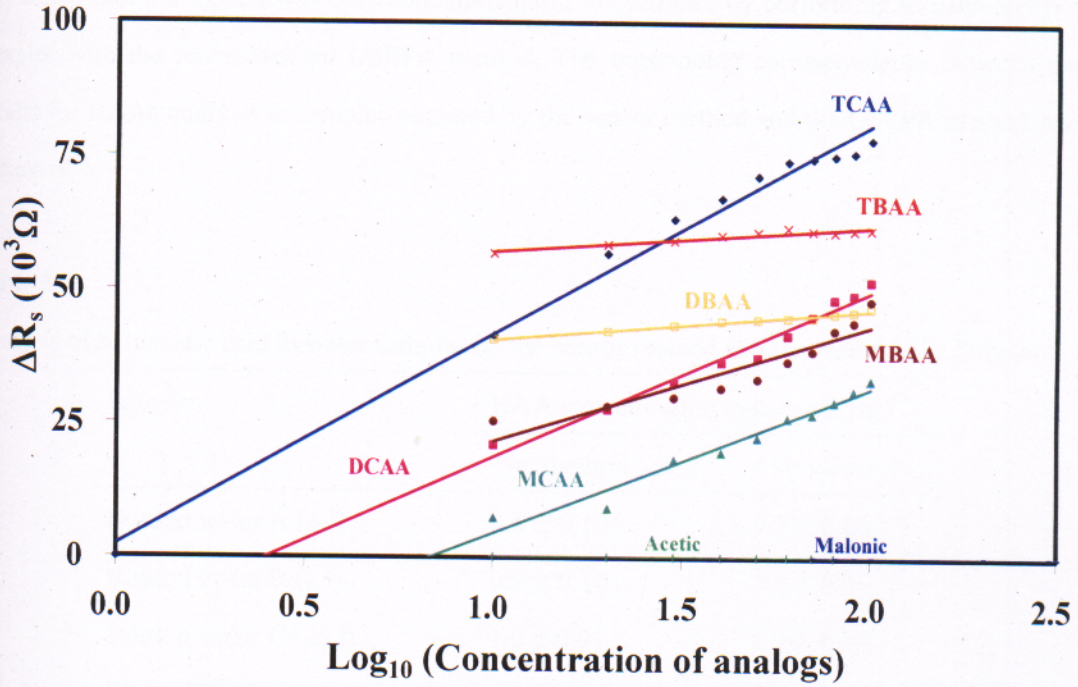

Fig. 3.16. Calibration curves for TCAA, DCAA, MCAA, TBAA, DBAA and MBAA obtained in the steady state on-line system using the developed MIP sensor.

3.4.4.8. Sample analysis

Determinations of haloacetic acid in four water samples, including three brands of commercial bottled water (1 and 25 l containers) and a domestic tap water (with home water treatment system) were performed using the conductometric sensor as a screening tool for haloacetic acid group. These water samples were assayed initially and directly. A corrected amount of measured HAA was compared with a calibration curve of TCAA alone, which was firstly prepared in range of concentration 0.5-10 $\mu g\ l^{-1}$. The exact concentrations of HAA in the samples acquiring from the assay by using conductometric sensor was verified by comparing through calibration curve obtained from recommended method of USEPA, LLE–GC–ECD (method 552.2)(USEPA, 1995), for analysis of HAAs in water. The results of each HAA amount in each samples assayed by using the sensor and the method 552.2 are classified in Table 3.2. It was found that the TCAA was only contaminated in the samples by performing measurement of samples with the recommended USEPA method. The outstanding correspondence between the results for HAAs analysis in samples obtained by the sensor method and the USEPA method was achieved.

Table 3.2

Analysis of haloacetic acid in water samples by the sensor method and the method 552.2 method

Sample	HAA concentration measured ($\mu g\ l^{-1}$)	
	The method 552.2	The sensor
Bottled water A (1 l)	0.8 ± 0.10	0.7 ± 0.00
Bottled water B (1 l)	0.9 ± 0.10	0.6 ± 0.01
Bottled water C (25 l)	1.0 ± 0.01	0.8 ± 0.00
Water filtration system (home)	1.2 ± 0.07	1.2 ± 0.02

For evaluating the recovery capability of proposed sensor, the water samples spiked with severally increased concentration of TCAA (30, 60 and 90 $\mu g\ l^{-1}$) either TCAA or a mixture of six HAAs (4.5, 9 and 14 $\mu g\ l^{-1}$ each HAA, total 27, 54 and 84 $\mu g\ l^{-1}$) was used as representative samples subjecting to the resistance measurement by MIP sensor.

Recovery data for these HAAs measuring with developed sensor are manifested in Table 3.3. As can be seen that the MIP sensor revealed the recovery capability in range of 99 and 105% and R.S.D. values less than 2% with bottled water A, B and C, and domestic tap water spiked with a standard solution of TCAA or total six HAAs at concentration level of 30, 60 or 90 $\mu g\ l^{-1}$, suggesting that accuracy of HAAs measurement by this sensor was good. The results also showed that for each water sample the recoveries percentage of TCAA-spiked samples was higher than that of HAA-spiked samples at all concentration of analyte studied. This was assumably because the generation of TCAA-imprinted sites within MIP was more complementary with TCAA than the other analogs, leading to better fit into imprint cavity in case of former molecule than the structurally related analogs containing in HAA mixture. These results eventually showed that the developed sensor can be efficiently employed to measure the amount of haloacetic acid disinfection by-products in the real-life samples.

Table 3.3

Recovery data from analysis of haloacetic acids in water samples after spiking with TCAA at various concentrations by the sensor method

Sample	Concentration of HAA in Water sample[a] ($\mu g\ l^{-1}$)	Measured[b] ($\mu g\ l^{-1}$) after adding TCAAs (%Recovery)		
		$\mu g\ l^{-1}$ added (TCAA)[c]		
		30.04	60.56	90.39
Bottled water A (1 l)	0.8±0.10	31.1±1.0 (101 ± 1)	61.4±1.2(100±1)	95.1±2.1(104±2)
Bottled water B (1 l)	0.9±0.10	31.4±0.72(102±0.0)	63.4±1.7(103±1)	94.3±1.5(103±1)
Bottled water C (25 l)	1.0±0.01	31.0±0.61(100 ± 1)	62.2±0.92(101±1)	94.0±2.4(103±1)
Water filtration system (home)	1.2±0.07	32.1±0.92(103±0.0)	63.6±0.91(103±1)	94.0±1.4(103±1)

Table 3.3 (Continued)

Sample	Concentration of HAA in water sample[a] ($\mu g\ l^{-1}$)	Measured[b] ($\mu g\ l^{-1}$) after adding HAAs (%Recovery)		
		$\mu g\ l^{-1}$ added (total six HAAs)[d]		
		30.04	60.56	90.39
Bottled water A (1 l)	0.8±0.10	27.3±0.56(100±0.0)	58.8±2.2(105±2)	87.8±1.6(104±1)
Bottled water B (1 l)	0.9±0.10	27.6±0.62(100±0.0)	57.9±1.2(103±2)	85.5±0.69(101±1)
Bottled water C (25 l)	1.0±0.01	27.6±0.41(100±0.0)	57.9±0.84(103±1)	88.9±1.7(105±1)
Water filtration system (home)	1.2±0.07	27.5±0.25(99±0.0)	57.5±0.83(102±1)	87.2±1.4(103±1)

[a] HAA concentration measured by the USEPA method 552.2 (mean S.D., n =3). Note that only TCAA was detected in all smples.
[b] Mean value R.S.D. (n = 3). The value in parenthesis is mean percent recovery of three indepedent measurements using only one electrode.
[c] Total six HAAs refers to TCAA, DCAA, MCAA, TBAA, DBAA and MBAA altogether.
[d] Expected concentrations are amounts added plus the amounts already present in the water sample.

3.3. Trichloroacetic Acid Imprinted Polypyrrole Modified Interdigitated Conductometric Sensor

3.3.1. Objectives

To find the promising determination method for haloacetic acids in drinking water with the use of polypyrrole imprinted with trichloroacetic acid as recognition element and inter-digitated conductometric transducer as sensing system.

3.3.2. Method

3.3.2.1. Immobilisation of TCAA-imprinted polypyrrole on the surface of the transducer

The immobilisation of TCAA-imprinted polypyrrole on surface of the IDC transducer was performed by means of a Coulostat at room temperature (25±1°C). For this purpose, the electropolymerisation of pyrrole was conducted on Coulostat galvanometer at a current density of $2x10^{-1}$ μeq sec^{-1} for 50 s in an aqueous solution containing 0.1 M pyrrole and 0.1 M TCAA, under a nitrogen atmosphere. The non-imprinted polymer (NIP) films, which were employed as controls, were prepared in the same manner as the MIP films but using 0.25 M KCl instead of 0.1 M TCAA for improving electrical sensitivity in NIP solution. The coated electrode was subsequently washed with 5 portions of 50 ml de-ionized water for at least 3 h to extract the template molecules.

3.3.2.2. Analytical detection of analyte

The chemical interaction of the prepared TCAA-MIPpy film with TCAA and its analogs was evaluated using interdigitated conductometric analysis. Optimized conditions for preparation of the polymers and for rebinding measurements were identified before evaluation of the sensor recognition properties for each MIP film. In addition, calibration data for both the developed interdigitated conductometric analysis system were determined, by incorporation of the TCAA-MIPpy film as means of detection. The coated-IDC electrode was fabricated in a self-made measuring cell with a 100 μl volume (Fig. 3.1C). Sample solution (2 ml) was pumped sequentially at a flow rate of 2 ml/min through a thermostat set at 25°C and then into the measuring cell which contained IDC sensor. The conductometric measurements were made on a precision LCR meter connected with a lab-top computer. The resistance data was processed using developed in-house software. All measurements were carried out in de-ionised water at room temperature (~20°C). The resistance measurement of the IDC sensor was performed by applying an alternating potential (100 mV) to the electrodes with an optimised frequency of 3 KHz. An

initial measure of the electrical resistance of the sensors was recorded with deionised water as a reference. The resistance change of the TCAA-imprinted pyrrole was measured as a function of the changes in the resistance of the polymer upon exposure to TCAA or other HAA analogs at concentrations from 1 to 120 $\mu g\ l^{-1}$. A series of standard solution of TCAA and analogs (1-130 $\mu g\ l^{-1}$) were added to the test solutions. Signal response of the sensor towards the analyte was reported as $1/\Delta R$, where $1/\Delta R$ is the conductivity shift response of the MIP electrode exposed to each sample solution, where ΔR is obtained from the change in resistance response as different, increasing, amounts of analyte are added.

3.3.2.3 The USEPA (method 522.2) (USEPA, 1995)

A 40 mL volume of sample is adjusted to pH <0.5 and extracted with 4 mL of methyl-tert-butyl-ether (MTBE). The haloacetic acids that have been partitioned into the organic phase are then converted to their methyl esters by the addition of acidic methanol followed by slight heating. The acidic extract is neutralized by a back extraction with a saturated solution of sodium bicarbonate and the target analytes are identified and measured by capillary column gas chromatography using an electron capture detector (GC/ECD). Analytes are quantitated using procedural standard calibration.

3.3.3. Material and equipment

3.3.3.1. Material

Polydimethyl-siloxane and hardener (Sylgard 184) were obtained from Dow Corning Corporation (MI, USA).

Trichloroacetic acid (TCAA) was purchased from Merck K.G. (Darmstadt, Ger-many). Dichloroacetic acid (DCAA), monochloroacetic acid (MCAA), dibromoacetic acid (DBAA), monobromoacetic acid (MBAA), tribromoacetic acid (TBAA) and malonic acid were obtained from Fluka Chemie AG (Buchs, Switzerland).

Analytical grade pyrrole was purchased from Fluka Chemie AG (Buchs, Switzerland) and its chemical structure is displayed in the Fig. 3.17.

Fig. 3.17. The chemical structure of conducting monomer used to prepare polypyrrole film

All chemicals for preparing buffer solution (K_2HPO_4, NaH_2PO_4, NaCl, HCl and KCl) were analytical grade and were obtained from Merck (Darmstadt, Germany).

All solvents used in this work were analytical grade and were dried with 4 A pore sized molecular sieve before use. Working standard solutions were prepared daily.

3.3.3.2. Equipment

Atomic force microscope (AFM) (Digital Instru-ments Inc., Santa Barbara, CA) (Fig. 3.18) using a Nanoscope III Scanning tunnel microscope was used to inspect the morphology of deposited film. AFM (Digital Instruments, CA, USA) with a Nanotec Electrinica WSxM scanning probe microscopy software version 3.0 Beta 8.1 (Digital Instruments, CA, USA) was utilized to determine the thickness of the films scratching with a needle and measuring depth of the scratches.

HP 4254A Precision LCR meter (Hewlett Packard, Germany) (Fig. 3.19) was employed to measure the electrical resistance of the thin-films polymer coated electrode.

Ismatec peristaltic pump (MCP-Process Series, Ismatec SA, Wertheim-Mondfeld, Germany) was used to drive the sample solution into the flow cell (Fig. 3.20).

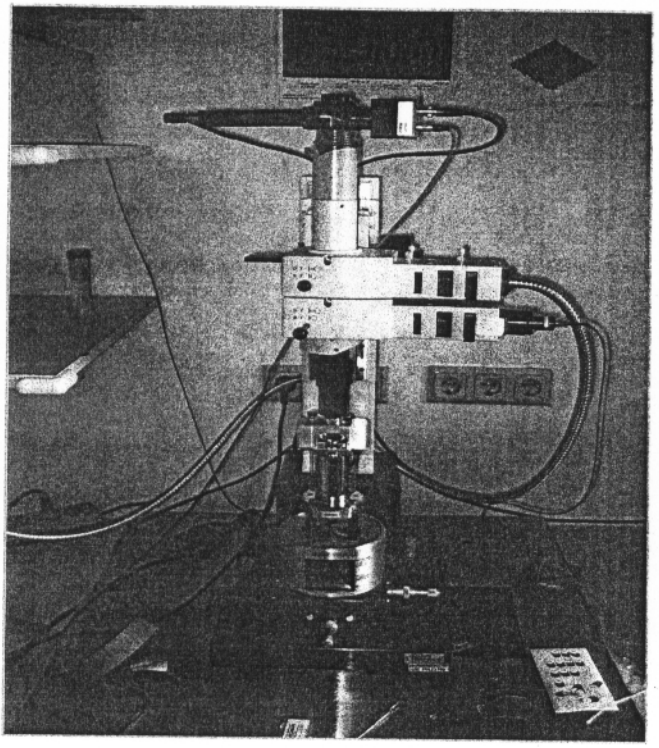

Fig. 3.18. Atomic force microscope (AFM)

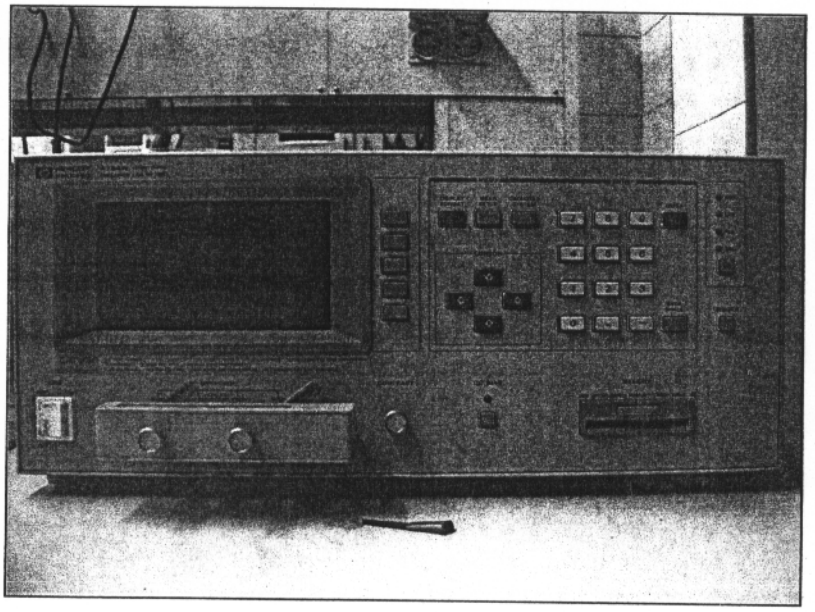

Fig. 3.19. A HP 4254A Precision LCR meter

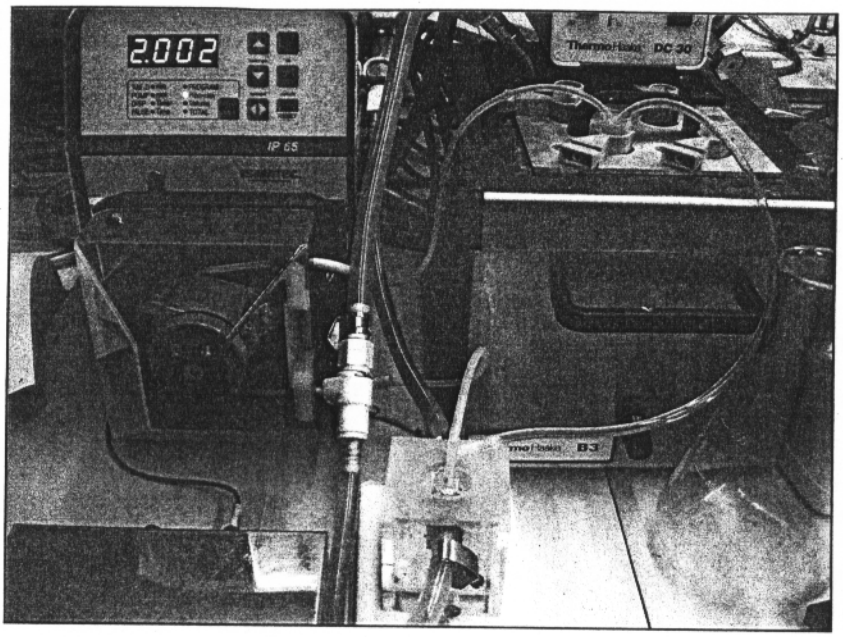

Fig. 3.20. A MCP-Process Series Ismatec peristaltic pump

3.3.4. Results and discussion

3.3.4.1. Preparation of TCAA-imprinted polypyrrole films

Pyrrole can be polymerized with an oxidation reaction electrochemically and chemically. The quality of the polymer can be greatly influenced by parameters such as counter ions, pH of reaction medium and temperature (Careem et al., 2006; Wu and Pawliszyn, 2004; Lehr and Saidman, 2006; Wen *et al.*, 2001). TCAA, a strong acid ($pK_a = 0.69$), which was employed as the template in this study, allowed the production of an imprinted polymer film of pyrrole with conducting properties. During the imprinting, the pyrrole monomer would be expected to incorporate a trichloroacetate anion to compensate cationic charge carried by the backbones of polypyrrole produced. After the removal of TCAA molecules by washing, a cavity with shape and size complementary to TCAA is created within the network of the polypyrrole film, presumably at the surface. The effect of thickness of polypyrrole film produced on electrodes may affect the efficiency of re-binding of template, thus affecting the signal response of the sensor.

3.3.4.2. The MIP-base electrode optimisation of preparation condition and polymer composition

In order to know how parameters, *i.e.,* current density, deposition time, and polymer composition, affected polymer properties, it was necessary that these parameters were explored. Current density was employed to attract monomer molecule to electrode surface. At which redox reaction of monomer and electrode surface commenced, the layer height of conducting polymer was ordinary controlled by the level of current density used (Gimenez-Romero *et al.*, 2006). Therefore, the degree of signal response of the prepared sensor was subsequently directed by varied current density. Effect of current density used to prepare polymer layer on capacity shift is shown in Fig. 3.21.

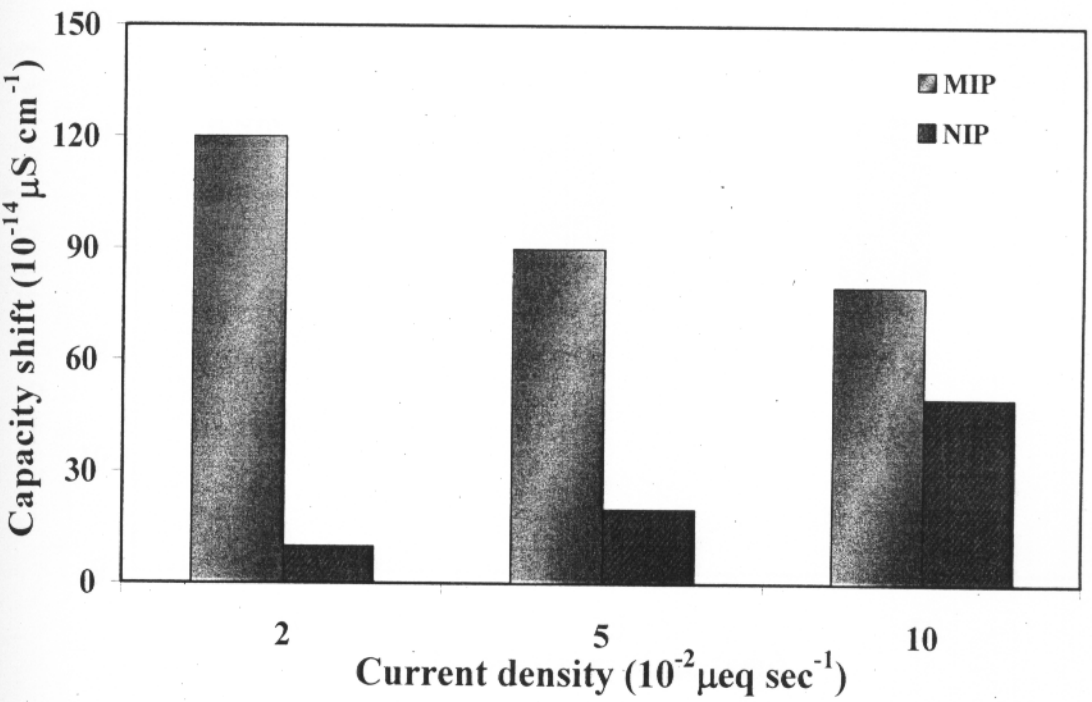

Fig. 3.21. Effect of current density in polypyrrole deposition process on the capacity shift using 1:1 of monomer-template mole ratio and 25 s of deposition time

It can be seen that higher current density employed the lower capacity shift was obtained. It may be because polypyrrole, which is a conducting polymer, can be changed the structure according to the density of the current (Albano and Sevilla, 2007). At low current

density, the prepared polymer probably was in an oxidized state and had positively charge backbone. In this state the anionic template can be attracted by the opposite charge of polymer to the binding site and hence, the signal transduction occurred. In contrast, the usage of too high current density the state of polymer structure may be more altered to the overoxidized state. In this state, there were negatively charge functional groups generating along the backbone. Such structure had a same charge with anionic form of the template ionized in aqueous binding solution. The recognition event was presumably prohibited from repulsion force between both negatively charge moieties. Finally, the capacity shift of the sensor was subsequently reduced.

Besides the current density, the deposition time is the other factor that can control the characterization of polymer layer and its effect on capacity shift of the sensor can be seen in Fig. 3.22.

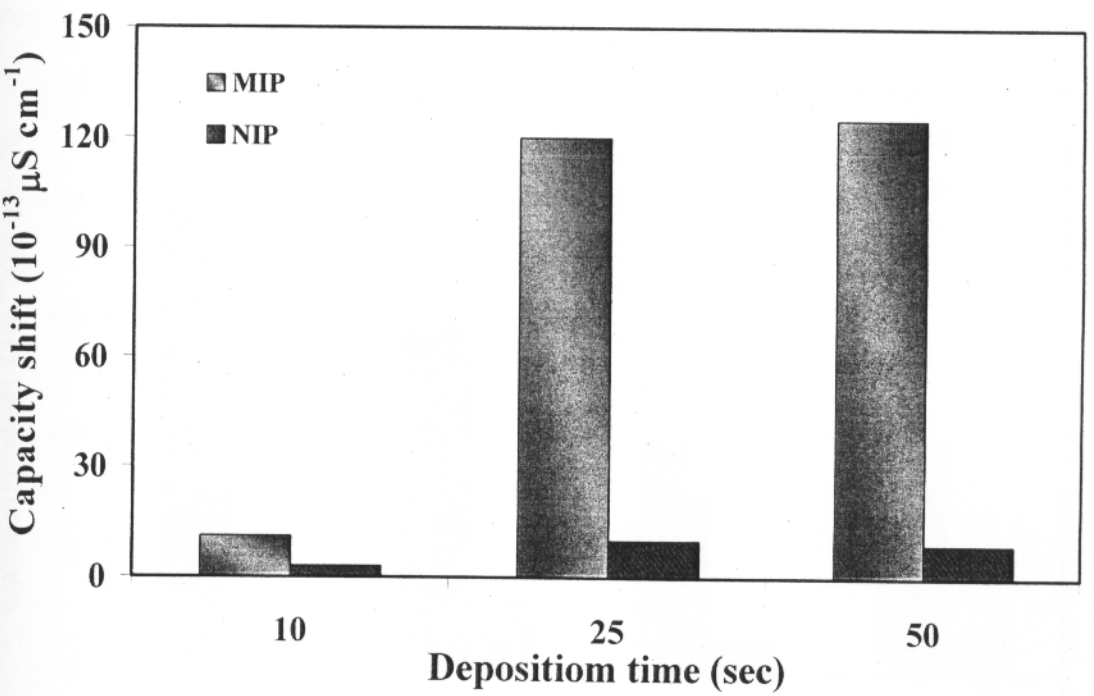

Fig. 3.22. Effect of deposition time in polypyrrole deposition process on the capacity shift using 2×10^{-2} µeq sec^{-1} of current density and 1:1 of monomer-template mole ratio

As can be seen, at initial time used to deposit polymer layer the capacity shift of the sensor was very low. Higher capacity shift response of sensor was received when using higher deposition time and capacity shift was level-off with deposition time longer than 25

s. This was possibly due to in an initial level of deposition time, the binding site and layer height of polymer was related directly. At low deposition time the polymer layer was generated as a thin film, in which a few recognition sites were produced. A much more amounts of recognition site were introduced inside polymer layer when increasing the deposition time. Too long deposition process, resulting in polymer layer thicker, may not produce the available binding site inside the layer. At which template molecule could not include owing to more difficult for diffusion process of template through dense network of polymer.

A good recognition site should attract and screen the analyte before allowing into the site. This manner could be obtained with the use of functional monomer and template which can interact to form a complex via their functional groups before being polymerized. The effect of mole ratio of these two components was therefore investigated in order to find the optimized ratio for the use in polymer preparation as can be seen in Fig. 3.23 below.

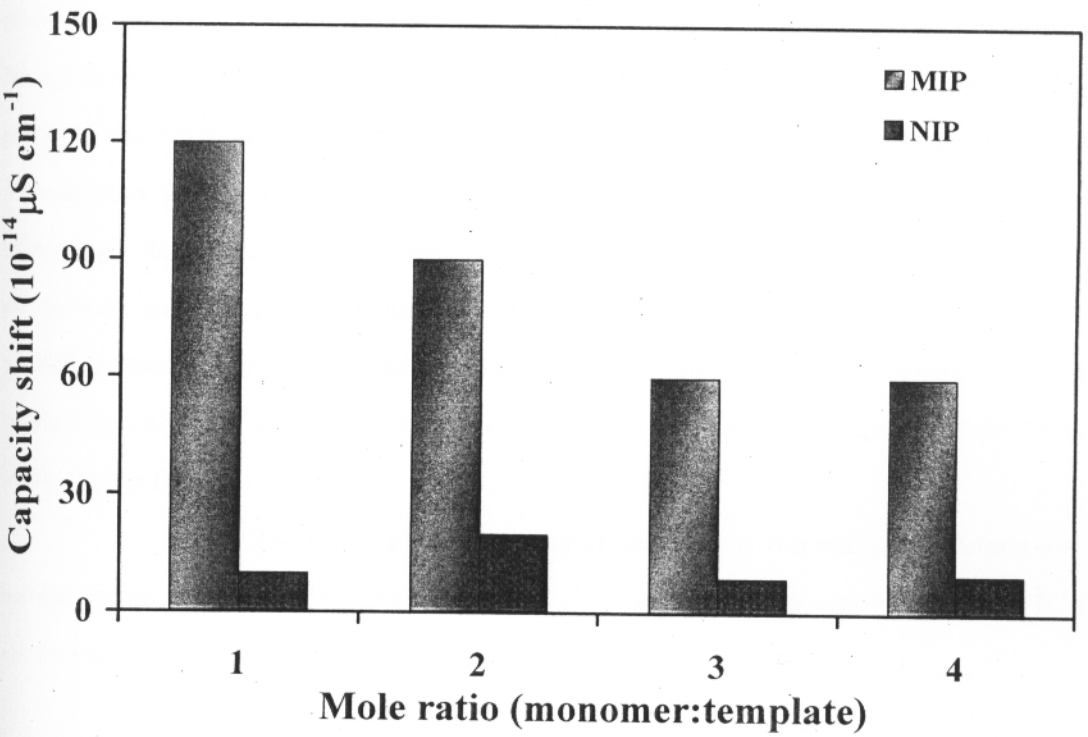

Fig. 3.23. Effect of monomer-template mole ratio used in polypyrrole deposition process on the capacity shift using 2 x 10^{-2} µeq sec^{-1} of current density and 50 s of deposition time

It was found that the capacity shift response of the sensor decreased with an increase in monomer-template mole ratio. It may be because pyrrole compound which behave as concurrently functional monomer and cross-linker. Increasing the amount of pyrrole can be considered as an increase in cross-linker amount, by which the denser network of polymer layer could be produced. This characteristic inhibited the inclusion of template to the binding site inside the layer. Thus, the capacity shift response of the sensor was decreased.

3.3.4.3. Influence of technological parameters on resistance shift response of polymer coated sensor

Miniaturized planar electrodes or interdigitated conductometric (IDC) transducers have become important electronic transducers in medical, biological and environmental diagnostics. This electronic transducer system is usually of compact design, easy to use, inexpensive and portable. In a sensor constructed with IDC, the sensitive layer is coated on the electrode of the transducer. The close proximity of the sensing element to the transducer enhances the response time, leading to rapid measurement due to low diffusion times. The incorporation of TCAA-imprinted polypyrrole into a IDC sensor would be expected to show high sample throughput, so that single measurements could be delivered in real time. Since the polypyrrole used for the construction of MIP has a conductive property, and factors such as applied frequency, temperature and electrolytes can have an effect on the conductivity of the conducting polymers, variation in these factors may affect the signal response of the TCAA-MIPpy on the IDC.

The results of measurement of conductivity responses of the electrodes at various current frequencies ranging from 20 Hz to 1 MHz when exposure to 100 $\mu g\ l^{-1}$ TCAA solution is shown in Fig. 3.24.

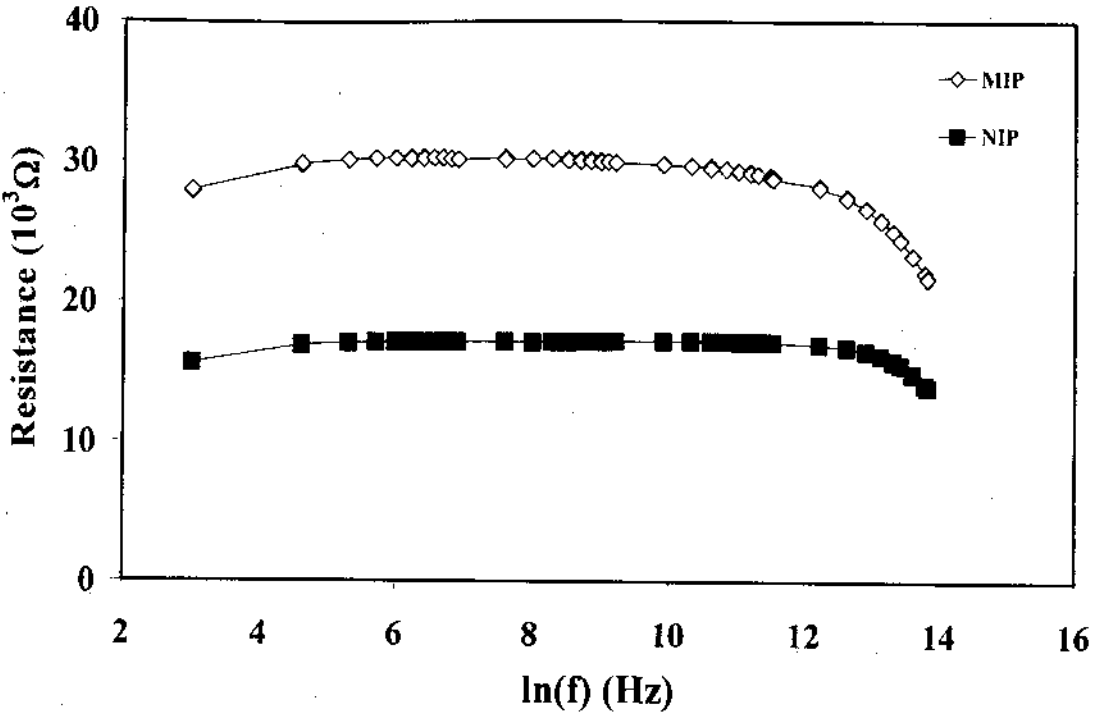

Fig. 3.24. Effect of applied frequency on resistance response of polypyrrole modified IDC sensor incubated with 100 ppb TCAA

It was found that resistance of MIP and NIP-coated electrodes were constant in a broad range of applied frequency. Resistance of both modified electrodes began to decrease with the use of high region of frequency. It was probably owing to at high applied frequency the channels or pores inside polymer network trended to extend which more allowed the conductive ionized water molecules can closely penetrate to contact with electrode surface. Resistance of the coated electrodes was therefore reduced. And when comparing resistance difference between MIP and NIP-coated electrode, a reasonable signal sensitivity of the sensor was obtained in the lower frequency region, rather than in higher frequency region. Additionally, at high frequency region a risk of the coated sensor to be destroyed was high, all subsequent measurements were therefore performed at an operating frequency of 3 KHz.

In general, the pyrrole polymer material has a conductive property due to electrical charge transfer within its network (Hallik *et al.*, 2006). Thus, the conductivity of the TCAA-MIPpy coated electrode can change as temperature varies. The conductivity responses of the TCAA-MIPpy and NIPpy coated electrodes at temperatures between 299 K and 333 K is

shown in Fig. 3.25 and 3.26, respectively. It can be seen that both polymer-coated electrodes were affected with temperature variation. An increase in temperature the lower resistance of both electrodes was obtained. This resistance reduction can be clearly observed in case of NIP-coated electrode about two folds higher than that of MIP-coated electrode. Normally, the material that can conduct electrical charge it can currently conduct the thermal energy. The increased heat from the environmental solution can be transferred into the polymer layer which caused the channels and pores expanded. This allowed the ionized water molecule or even template easily diffused to the electrode surface. Resistance of coated sensor was then reduced. This suggested that measurement of the pyrrole-based electrode had to be therefore carried out under controlled fixed temperature.

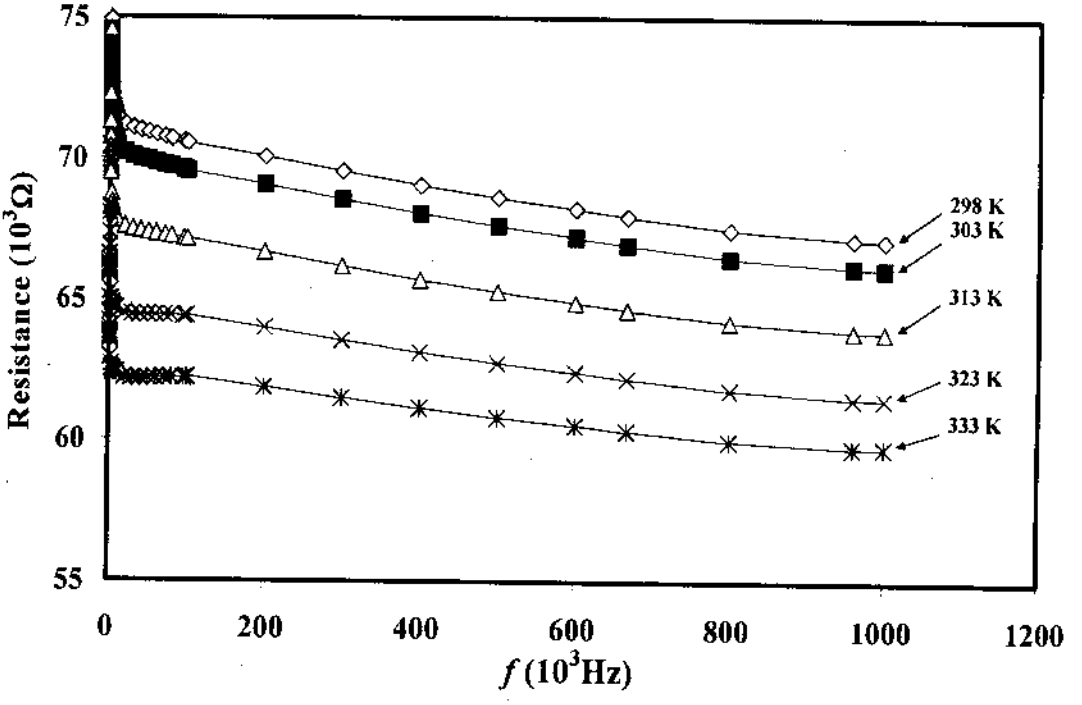

Fig. 3.25. Effect of temperature on resistance response of TCAA-imprinted polypyrrole incubated with 100 ppb TCAA

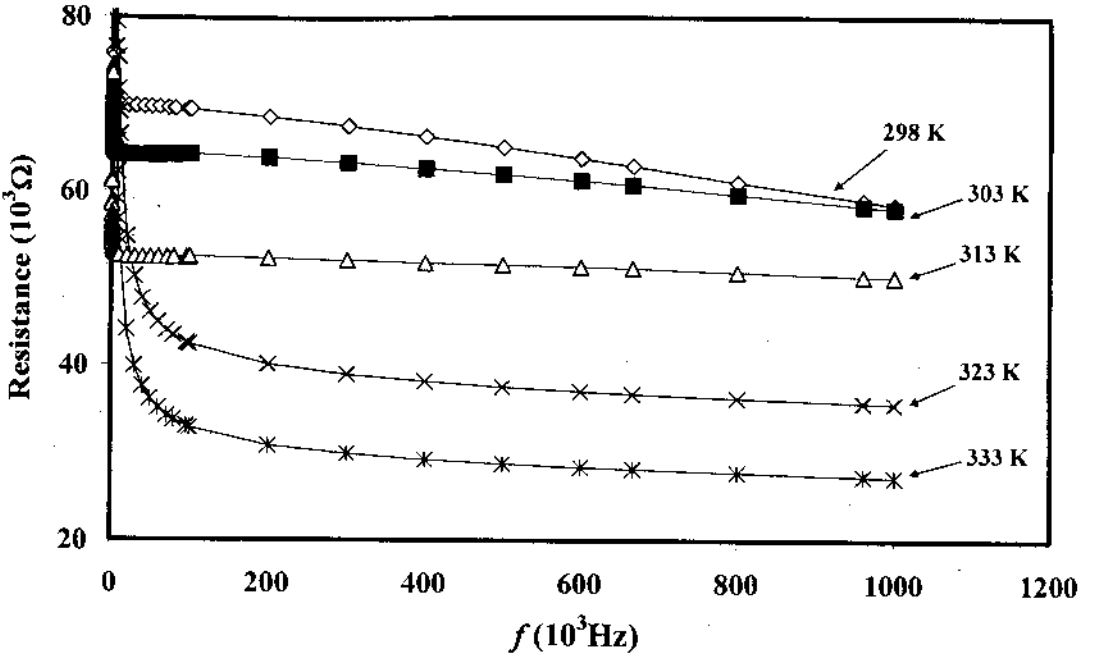

Fig. 3.26. Effect of temperature on resistance response of non-imprinted polypyrrole incubated with 100 ppb TCAA

The Arrhenius plot of signal response of the MIP sensor and measured temperature show a clear temperature dependency of the sensor as same the other polymer material, imprinted poly(EDMA-*co*-VPD), as can be seen in Fig. 3.27. But, the activation energy calculated from the plot (3.5 kcal mol^{-1}) of imprinted polypyrrole was lower than imprinted poly(EDMA-*co*-VPD). This revealed the more easy formation of charge-transfer complexes in case imprinted polypyrrole. Additionally, the calculated slope of imprinted polypyrrole's Arrhenius plot showed lower magnitude when compared with imprinted poly(EDMA-co-VPD). It suggested that the imprinted polypyrrole demonstrated lower sensitivity on changed temperature than the latter one. From the results obtained, this polymer was also recommended to perform measurement in the good controlled condition for avoiding from temperature interfering.

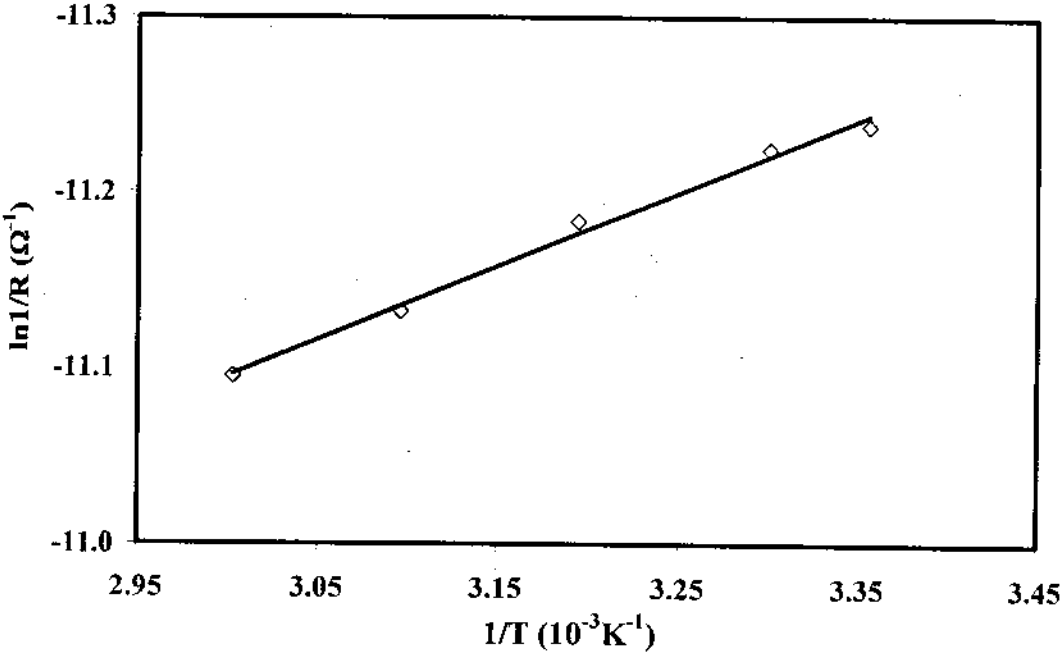

Fig. 3.27. Arrhenius plot for the electrical conductivity of TCAA-MIP sensor.

3.3.4.4. Effect of ionic substances in solution background on the resistance shift response of polymer coated sensor

Measurement of signal response of this sensor intended to be carried out in aqueous medium. In nature, it is undoubtedly possible that there may be some contaminants exited together with interested analyte (Sultan and Gabryelski, 2006). In order to know how big the effect of these contaminants was, the various types of solution background were examined. It can be seen in Fig. 3.28, the resistance change response of MIP and NIP-coated sensor was influenced in all buffer solution selected. Effect of template concentration dependence of signal response of MIP and NIP-coated electrodes was completely diminished. It was presumably due to the anionic ion of these inorganic substances exited in solution may lead to the formation of charge-neutral contact ion pairs with cationic species in polypyrrole backbones, which do not contribute to conductivity.

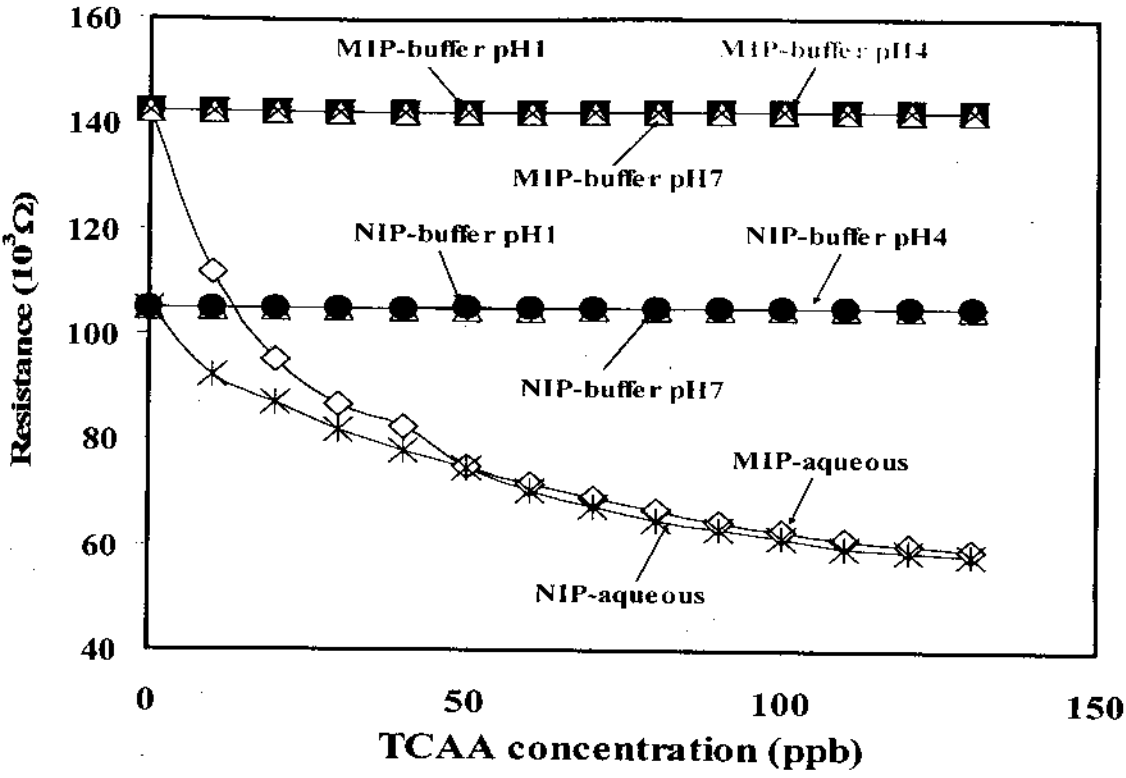

Fig. 3.28. Effect of solution background on the resistance changes of polypyrrol modified IDC sensor.

In aqueous solution background, in which there was no high concentration of foreigner ionic substances, both MIP- and NIP-coated sensor clearly showed the concentration dependence of sensors to the incremental addition of TCAA. This suggested that the signal response measurement of the sensor should be performed in an aqueous environment.

The effect of the common electrolyte, NaCl on the signal response of IDC sensor was also investigated as can be seen in Fig. 3.29. The signal responses of the MIP-coated IDC sensor for water solutions containing NaCl salt between 1-30 g l^{-1} (0-500 mM) were measured under the optimized conditions. Increasing concentrations of NaCl in sample solutions containing 100 μg l^{-1} TCAA resulted in the increased conductivity response of both MIP- and non-MIP-coated electrode. Indeed, the conductivity behaviour of TCAA-imprinted polypyrrole in the presence of NaCl salt is similar to that of the poly (vinyl chloride) membrane bearing the TCAA-imprinted poly(vinylpyridine-*co*-ethyleneglycoldimethacrylate) particles in the previous

work (Suedee *et al.*, 2004), and which had an ionic conductivity similarly to polymeric solid electrolytes.

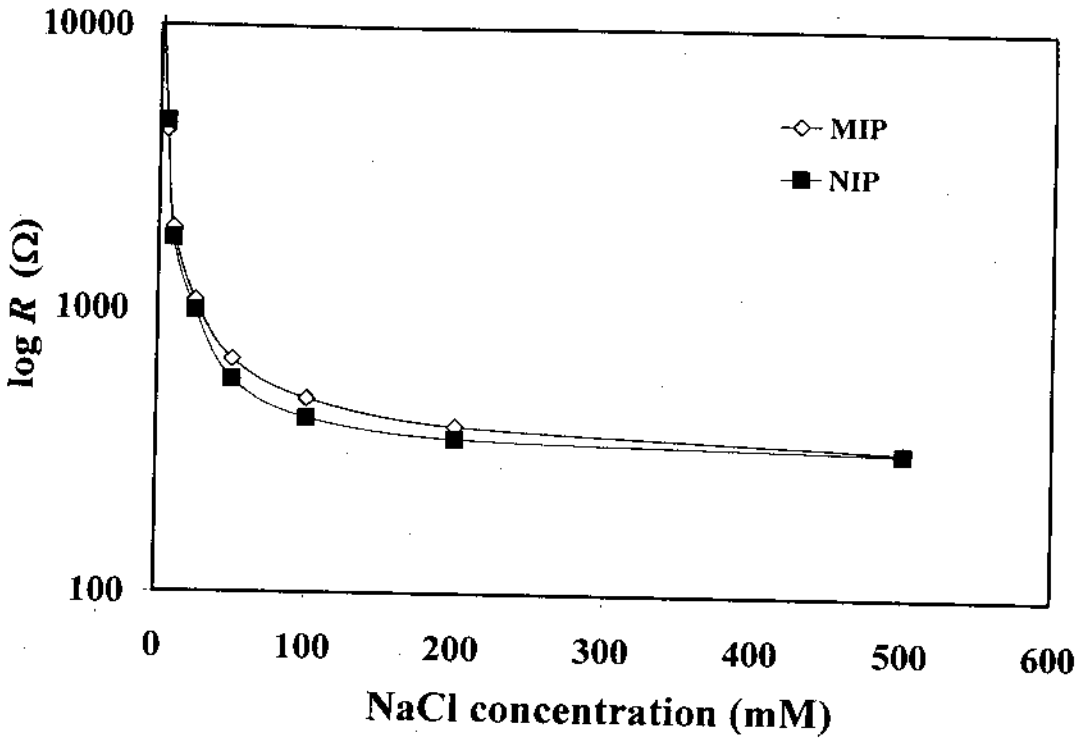

Fig. 3.29. Effect of NaCl concentration on resistance response of imprinted polypyrrole incubated with 100 ppb TCAA.

The mobility of the Na^+ ions coupled with the segmental motion of the non-cross-linked polypyrrole chains, could be a reason for the increase in conductivity of the film in the presence of excess NaCl salt. Independency of addition of the electrolyte upon signal responses of MIP sensors with NIP sensors was observed only at low concentrations of NaCl (< 1 mM). Thus, measurements using the pyrrole-based electrode should be carried out under low concentration of Na^+ ion.

3.3.4.5. Concentration dependence of conductivity shift response of the polymer coated sensor

The concentration dependency of the prepared sensor was examined by using template concentration in the range of 0-130 ppb and the measurement was performed at ambient temperature. As can be seen in the Fig. 3.30, increasing the template concentration up to 50 ppb the capacity changes response of the imprinted sensor sharply increased. At template concentration more than 50 ppb, the resistance change response was gained to the level off state.

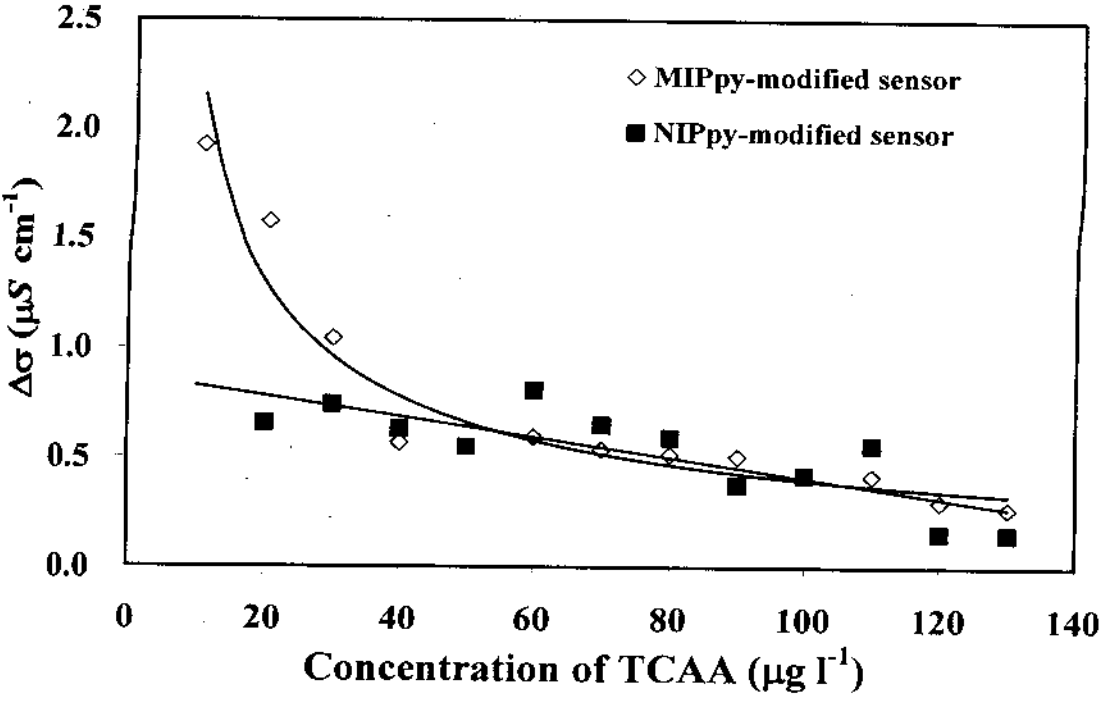

Fig. 3.30. Conductivity changes of (a) the TCAA-MIPpy coated IDC in comparison to (b) the non-imprinted polymer coated electrode at various concentrations of added TCAA.

The much difference of the signal response between imprinted sensor and reference sensor was observed in the concentration range of 0-50 ppb. It was possibly due to at initial range of template concentration the recognition sites existed in the polymer matrix were responsible for the rebinding process and hence, for the signal response of the sensor. At the template concentration higher than 50 ppb the saturation of recognition cavities may be occurred

and the considerable amount of non-specific binding might be responsible for the resistance change response of the sensor. The changing in the surface conductivity of the polypyrrole material could explain for the increase in the conductivity signal of the MIP film (after polymerisation) when exposed to TCAA in water solutions. The binding of the template molecule to the MIP might be expected to result in an increased continued transduction phase of the non-cross-linked polypyrrole through charge-transfer complex interaction (Chakrabarti *et al.*, 2002).

3.3.4.6. Selectivity and analytical characteristics of polymer coated sensor

Specificity of the TCAA-imprinted polypyrrole coated IDC in the presence of analogs was examined, using TCAA, five structurally analogs (DCAA, MCAA, TBAA, DBAA and MBAA) and two non-structurally related analogs (acetic and malonic acid). Fig. 3.31 below shows the conductivity shift responses of the MIP coated electrode to the haloacetic acid and non-haloacetic analogs.

5 HAA analogs in the 1-130 $\mu g\ l^{-1}$ concentration range generated small changes in the electrical conductivity signal of the MIP coated electrode. The two non-structurally related analogs in the 1-130 $\mu g\ l^{-1}$ concentration range showed little or no change in the electrical conductivity signal of the MIP coated electrode. These results demonstrated that the MIP selectively recognized the TCAA template on the interdigitated conductometric transducer. Although the HAA analogs used for this study contained halogen-substituted carboxylic acid groups as the template, they also contained different halogen atoms and different degree of substitution, which caused them not fit properly to the TCAA-imprint sites in the MIP, and hence, a charge-transfer complex was not formed, thereby no transduction signal generated.

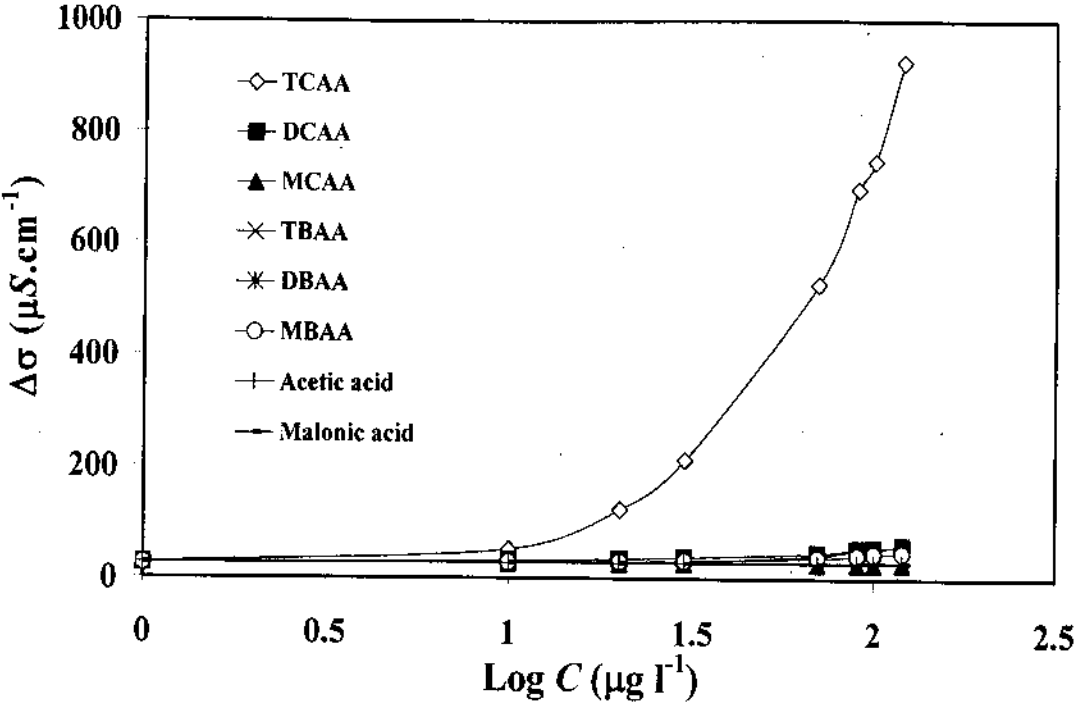

Fig. 3.31. Conductometric responses for TCAA-MIPpy coated IDC at various concentrations of TCAA and analogs.

The calibration characteristics of the sensor fabricated with imprinted polypyrrole were identified as can be seen in Table 3.4. The calibration graphs were obtained from the plot of signal response of the sensor versus the logarithm of concentrations of TCAA and its analogs. The calibration data are shown in Table. The linearity of all calibration data was determined in the HAA concentration range of 10-130 ppb. The concentration graphs of HAA are linear with a correlation coefficient higher than 0.966. The limits of detection obtained from extrapolation of the linear segment of the curve between the conductivity response ($1/\Delta R$) and the logarithm of the concentration showed the 10 - 120 $\mu g\ l^{-1}$ (ppb) sensitivity range of TCAA analyses using IDC analysis (see Table). The dynamic range for IDC analysis was narrower than that for CV analysis (0.1-1000 $mg\ l^{-1}$).

Table 3.4

Calibration data obtained for the analysis of TCAA by the MIP sensor

Compound	Slope	R^2	Working range ($\mu g\ l^{-1}$)	LOD ($\mu g\ l^{-1}$)
TCAA	38.89	0.997	10-120	1.0

Furthermore, the specificity characteristics of TCAA-MIPpy shown on the IDC analyses, which were template specific, were different to those for the CV analyses. The assay time for the IDC was as fast as 3 min, and the MIP coated electrode is reusable at least 50 times without any change in its sensing property. Stability of the coated electrode was good when stores at room temperature in dry-air condition and the electrode can be used for longer than 1 month and retains the same sensor characteristics during this period.

3.3.4.7. Analysis of water samples

The TCAA-imprinted polypyrrole conductometric sensor was employed as an analytical tool for haloacetic acid group determination in four water samples, including three brands of commercial bottled water (1 and 25 l containers) and a municipal tap water obtained from home filtration system. These water samples were assayed directly. A calibration curve of TCAA alone was prepared in range of concentration 0.5-10 $\mu g\ l^{-1}$ and compared to that measured for HAA in the samples. A method for analysis of HAAs in water, LLE–GC–ECD recommended by the USEPA (method 552.2) was also used to verify the amounts of HAA in the samples as obtained by the conductometric sensor. The results obtained for analyses of each sample by the sensor and the method 552.2 are displayed in Table 3.5. The measurement of HAAs with the USEPA method revealed that only TCAA was contained in the samples. The results for HAAs analysis by the sensor method was in excellent agreement with that obtained with the USEPA method.

Table 3.5

Analysis of haloacetic acid in water samples by the sensor method and the method 552.2

Sample	HAA concentration measured ($\mu g\ l^{-1}$)	
	The method 552.2	The sensor
Bottled water A (1 l)	0.8 ± 0.10	0.8 ± 0.03
Bottled water B (1 l)	0.9 ± 0.10	0.8 ± 0.04
Bottled water C (25 l)	1.0 ± 0.01	1.4 ± 0.06
Water filtration system (home)	1.2 ± 0.07	1.8 ± 0.07

For validation purposes a recovery study was performed by spiking the above water samples with increasing amounts of either TCAA (30, 60 and 120 $\mu g\ l^{-1}$) or a mixture of six HAAs (5, 10 and 20 $\mu g\ l^{-1}$ each HAA, total 30, 60 and 120 $\mu g\ l^{-1}$). Recovery data for these analyses are summarized in Table 3.6.

Table 3.6

Recovery data from analysis of haloacetic acids in water samples after spiking with TCAA at various concentrations by the sensor method

Sample	Concentration of HAA in water sample[a] ($\mu g\ l^{-1}$)	Measured[b] ($\mu g\ l^{-1}$) after adding HAAs (%Recovery)		
		$\mu g\ l^{-1}$ added (TCAA)[c]		
		30	60	120
Bottled water A (1 l)	0.8±0.03	30.2±0.73(98±2)	59.4±0.65(98±1)	117.5±0.51(97±0.4)
Bottled water B (1 l)	0.8±0.04	30.3±0.12(98±0.4)	59.7±0.84(98±1)	118.5±0.65(98±0.5)
Bottled water C (25 l)	1.4±0.06	30.1±0.14(96±0.5)	58.6±0.24(95±0.4)	115.6±0.61(95±0.5)
Water filtration system (home)	1.8±0.07	30.1±0.17(94±0.6)	58.2±0.46(94±0.8)	114.6±2.11(94±2)

Table 3.6 (Continued)

Sample	Concentration of HAA in water sample[a] ($\mu g\ l^{-1}$)	Measured[b] ($\mu g\ l^{-1}$) after adding HAAs (%Recovery)		
		$\mu g\ l^{-1}$ added (total six HAAs)[d]		
		30	60	120
Bottled water A (1 l)	0.8±0.03	29.7±0.59(97±2)	58.5±0.40(96±0.7)	115.8±0.33(96±0.3)
Bottled water B (1 l)	0.8±0.04	29.7±0.62(96±2)	58.5±0.59(96±1)	115.9±1.6(96±1)
Bottled water C (25 l)	1.4±0.06	29.1±0.30(92±1)	56.7±0.38(92±0.6)	111.8±0.18(92±0.2)
Water filtration system (home)	1.8±0.07	29.8±0.47(93±2)	57.6±0.77(93±1)	113.3±1.6(93±1)

[a] Expected concentrations are amounts added plus the amounts already present in the water sample (mean ± R.S.D, $n = 3$)
[b] With home filtration system.
[c] Total six HAAs refers to TCAA, DCAA, MCAA, TBAA, DBAA and MBAA altogether.

As it can be seen recoveries range between 92 and 98% and S.D. values less than 2% were achieved with bottled water A, B and C, and municipal tap water spiked with a standard solution of TCAA or total six HAAs at concentration level of 30, 60 or 120 $\mu g\ l^{-1}$, indicating that accuracy of assay with the sensor is good. It was shown that the haloacetic acid disinfection by-products in the real-life samples can be effectively measured with the sensor.